Report

Current Biology

Food Reward Chemistry Explains a Novel Pollinator Shift and Vestigialization of Long Floral Spurs in an Orchid

Graphical Abstract

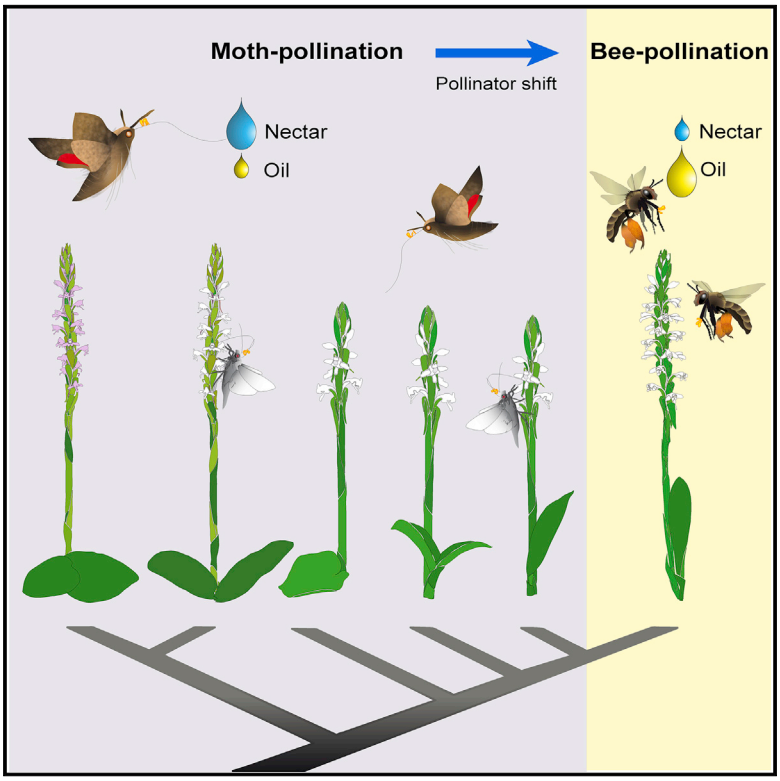

Highlights

- *Satyrium longicauda* is characterized by two pollination ecotypes
- Pollination by oil-collecting bees is derived from moth pollination
- The pollinator shift process is associated with pre-adaptation and vestigialization
- Minor modifications in floral chemistry can initiate major pollinator shifts

Authors

Miguel Castañeda-Zárate, Steven D. Johnson, Timotheüs van der Niet

Correspondence

vdniet@gmail.com

In Brief

Pollinator shifts were frequent in angiosperms, but how do they happen? Castañeda-Zárate et al. study "evolution-in-action" in an African orchid. They reconstruct a novel shift from moth- to oil-collecting bee pollination. The bee-pollinated form resembles moth-pollinated forms, but produces oil instead of nectar, driving the pollinator shift.

Castañeda-Zárate et al., 2021, Current Biology *31*, 1–9
January 11, 2021
https://doi.org/10.1016/j.cub.2020.10.024

CellPress

Please cite this article in press as: Castañeda-Zárate et al., Food Reward Chemistry Explains a Novel Pollinator Shift and Vestigialization of Long Floral Spurs in an Orchid, Current Biology (2020), https://doi.org/10.1016/j.cub.2020.10.024

Current Biology

CellPress

Report

Food Reward Chemistry Explains a Novel Pollinator Shift and Vestigialization of Long Floral Spurs in an Orchid

Miguel Castañeda-Zárate,[1,2] Steven D. Johnson,[1] and Timotheüs van der Niet[1,3,*]
[1]Centre for Functional Biodiversity, School of Life Sciences, University of KwaZulu-Natal, Pietermaritzburg, Carbis Road, Scottsville 3209, South Africa
[2]Twitter: @MCastanedaZ
[3]Lead Contact
*Correspondence: vdniet@gmail.com
https://doi.org/10.1016/j.cub.2020.10.024

SUMMARY

During the evolutionary history of flowering plants, transitions between pollinator groups (pollinator shifts) have been frequent,[1] and contributed to the spectacular radiation of angiosperms.[2] Although the evolution of floral traits during pollinator shifts has been studied in real time under controlled laboratory conditions,[3] it is challenging to study in nature and therefore poorly understood.[4–7] Using a comparative, multidisciplinary approach, we dissect the evolution of floral traits during a pollinator shift in the long-spurred African orchid *Satyrium longicauda*. Phylogenetic analysis and ecological experiments revealed a shift from moth- to oil-collecting bee pollination. Remarkably, flowers of the bee-pollinated form are similar in morphology, color, and overall volatile chemistry to those of moth-pollinated forms, but differ in having spurs that are mostly devoid of nectar, and have an elevated presence of the oil-derived compound diacetin, which oil-collecting bees use as a cue for oil presence.[8] Experiments demonstrated that long spurs are critical for pollination of a moth-pollinated form, but are not needed for pollination of the bee-pollinated form. We conclude that the pollinator shift in *Satyrium* was mediated by a switch in chemistry of the pollinator reward. The ancestral presence of diacetin might have served as a pre-adaptation for bee pollination, whereas the current mismatch between flower morphology and bees is due to the retention of vestigial floral spurs. These results elucidate the sequence of floral evolution in the early stages of pollinator shifts and help to explain the assembly of suites of co-varying traits through pre-adaptation and vestigialization.[9–12]

RESULTS AND DISCUSSION

Evidence for Pollination Ecotypes in *Satyrium longicauda*

Pollinator shifts occur when populations of the same species adapt to different pollinators.[13] This process results in the formation of pollination ecotypes.[5,14–16] Such ecotypes are characterized by intraspecific variation in floral traits and represent ideal model systems to investigate the evolutionary process underlying pollinator shifts. We discovered the presence of pollination ecotypes in *Satyrium longicauda*, a highly variable southern African grassland orchid that has its center of diversity in a global hotspot of biodiversity.[17] Only two subspecific taxa of *S. longicauda* are currently recognized,[17] but extensive fieldwork revealed the frequent co-occurrence of multiple discrete forms (see below). Studying ecotypes that occur in sympatry offers two great advantages over studying allopatric populations: sympatric co-occurrence (1) minimizes environmental causes of phenotypic differences and reveals their genetic basis[18] and (2) excludes the possibility that observed differences in plant-pollinator interactions reflect geographical turnover in pollinator assemblages[19,20] rather than differences in the function of floral traits. Within a circa 1 km^2 site, we identified six forms of *S. longicauda* that differ in floral traits including spur length and that can be unambiguously diagnosed by the number and position of their leaves and habitat (Figure S1; Table S1). Fruit set was absent when visitors were excluded for all six forms, whereas 70%–100% of cross-pollinated flowers set fruit, indicating pollinator dependence for all forms and confirming previous experiments done on one of the forms.[21]

Previous work has shown that flowers of the two most common forms of *S. longicauda* are pollinated by nocturnal moths.[22] Floral traits of all six forms conform to the syndrome of moth-pollination, including white, sweetly scented flowers with relatively long spurs.[23,24] Our initial hypothesis was therefore that all six forms are pollinated by nocturnal moths, but that variation in spur length could reflect pollination by moths with different tongue lengths.[25] To identify pollinators, we made direct observations and used motion-activated cameras with close-up lenses.[26] Five out of the six forms (*MOTH1–MOTH5*), were visited exclusively or predominantly by nocturnal moths, including hawkmoths (Sphingidae) and settling moths (Noctuidae), which carried pollinaria (Figure 1; Table S2; Video S1). For two of these forms (*MOTH1* and *MOTH3*), occasional visits

Please cite this article in press as: Castañeda-Zárate et al., Food Reward Chemistry Explains a Novel Pollinator Shift and Vestigialization of Long Floral Spurs in an Orchid, Current Biology (2020), https://doi.org/10.1016/j.cub.2020.10.024

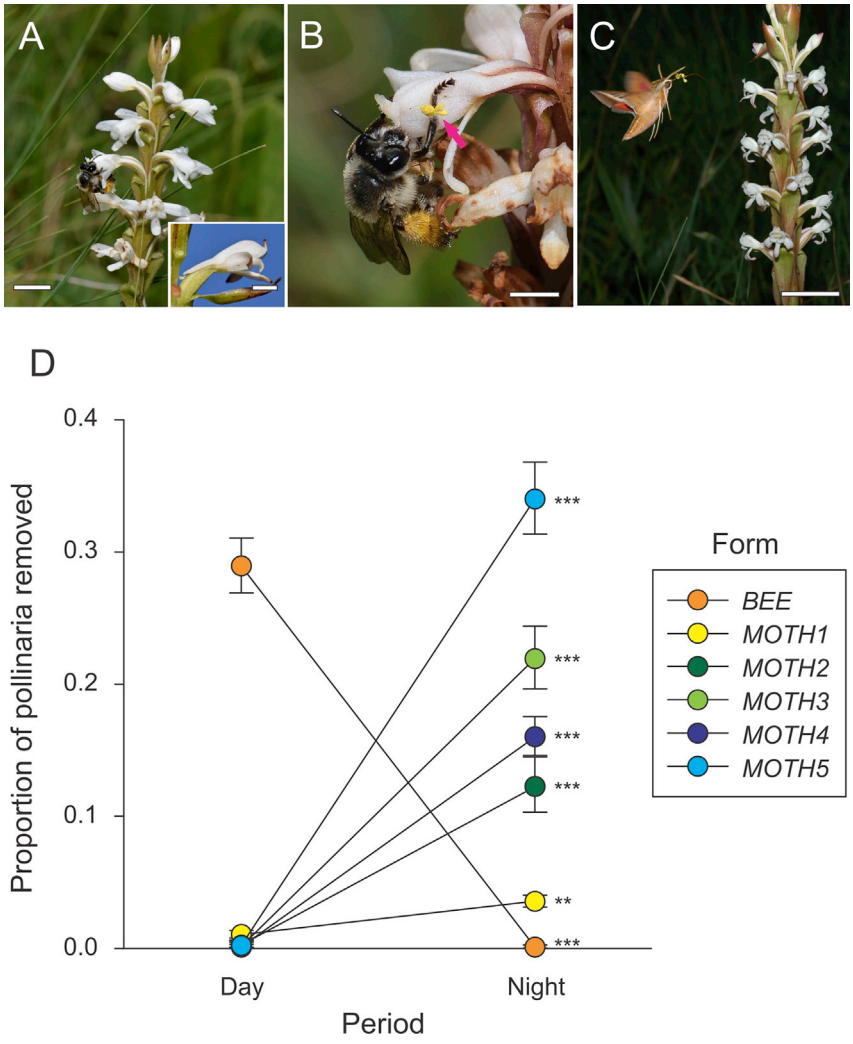

Figure 1. Pollinators of *Satyrium longicauda* and Pollinator Activity Times

(A) An oil-collecting *Rediviva neliana* bee visits a flower of the *BEE* form. The inset shows a flower of a rare mutant of the *BEE* form in which floral spurs are almost absent.

(B) *Rediviva neliana* with pollinaria attached to the tibia of its foreleg (pink arrow) and using its other foreleg to collect oil from a flower of the *BEE* form.

(C) The hawkmoth *Basiothia schenki* carries a load of pollinaria on its proboscis as it approaches an inflorescence of the *MOTH4* form.

(D) Comparison of the mean ± SE proportion of flowers with pollinaria removed during day and night periods (form × period $\chi^2_1 = 38.69$, $p < 0.001$)

***$p < 0.001$, **$p < 0.01$. Scale bars, 10 mm (A) and 5 mm (A inset), 5 mm (B), and 50 mm (C). Photo credits: SD. Johnson. See also Table S2 and Video S1.

by diurnal long-tongued nemestrinid flies were also recorded (Table S2). Contrary to our expectations, one form of *S. longicauda* (*BEE*) did not receive any nocturnal visits but was frequently (n = 134) visited by *Rediviva neliana* bees, of which 63.4% carried pollinaria (Figure 1; Table S2; Video S1). All of the 15 *R. neliana* individuals captured while visiting flowers were female, indicating a significant sex bias (exact binomial test: $p < 0.001$). Pollinator behavior and the pollination mechanism differed markedly between *MOTH* and *BEE* forms: moths inserted their proboscides into the spurs of *MOTH* forms while hovering in front of, or settling on, inflorescences, and pollinaria of these forms are attached to the proboscis (Figure 1; Video S1). In contrast, bees did not insert their proboscides into the *BEE* form but rather used their forelegs to probe the galeate labellum. Pollinaria (mean ± SD: 4.0 ± 2.70, range 1–12) were attached to the tibia of bees' forelegs (Figure 1; Video S1) (cf. Pauw[27]). The morphology, site of placement, and angle of orientation of these pollinaria differ from those of all other orchids pollinated by oil-collecting bees that occur in the area.[28]

To confirm the periodicity of pollination (in a manner independent of any observer- or trigger-bias that might influence direct observations and camera trapping, respectively), we also systematically compared pollinarium removal during diurnal and nocturnal intervals.[29] Results showed that pollinarium removal in the five *MOTH* forms is significantly higher at night than during the day, whereas pollinarium removal in the *BEE* form was exclusively diurnal (Figure 1). Natural fruit set among the 6 forms ranged from 79%–90%, indicating that pollinator visits contribute to fecundity.

Contrary to our initial prediction based on floral syndrome traits, these combined results suggest the existence of a bee-pollinated ecotype (*BEE*) that closely resembles the sympatric moth-pollinated (*MOTH*) ecotypes of *S. longicauda*, raising questions about which traits could mediate the partitioning of pollinators among these co-occurring ecotypes.

Functional Traits Associated with Two Pollination Ecotypes

The behavior of moths on flowers was consistent with nectar foraging. The behavior of bees, which involved insertion of their legs rather than their proboscides into flowers, was suggestive of a different foraging mode (Video S1). Female *Rediviva* bees visit flowers not only for nectar, but also to collect oil, which they collect with densely pilose forelegs.[30–32] These floral oils mostly consist of acetylated acylglycerols of fatty acids.[33,34] Observations of foraging behavior (visits exclusively by female *Rediviva* bees, insertion of front legs, extended duration of visits to individual flowers and visits to many flowers per plant) (Video S1), suggest that flowers of the *BEE* form produce floral oil.

To test *S. longicauda* flowers for the presence of oil, we used Sudan IV crystals.[35] As predicted, the inner surface of the labellum and spur entrance of flowers of the *BEE* form stained red, indicating the presence of fatty oil. However, flowers of the five *MOTH* forms stained similarly (Figure S2). To further explore the presence of floral oil-derived compounds, we

Please cite this article in press as: Castañeda-Zárate et al., Food Reward Chemistry Explains a Novel Pollinator Shift and Vestigialization of Long Floral Spurs in an Orchid, Current Biology (2020), https://doi.org/10.1016/j.cub.2020.10.024

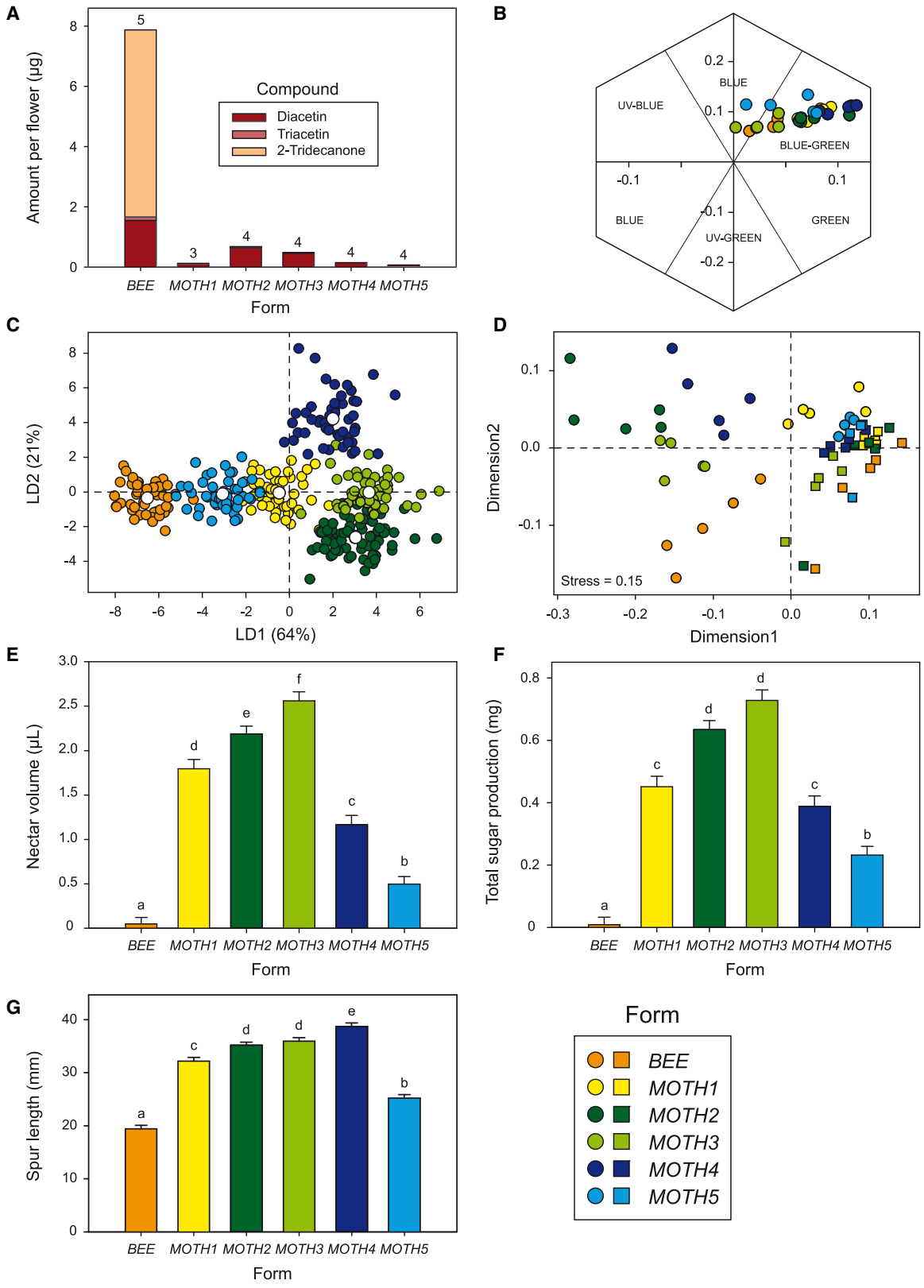

Figure 2. Functional Floral Traits of *Satyrium longicauda*

(A) Production of acetylated glycerols and 2-tridecanone among six forms. Sample sizes are given above each bar.

(B) Flower (labellum) color plotted in the bee-vision model, showing that the flower color of the *BEE* form overlaps with that of various *MOTH* forms.

(legend continued on next page)

Please cite this article in press as: Castañeda-Zárate et al., Food Reward Chemistry Explains a Novel Pollinator Shift and Vestigialization of Long Floral Spurs in an Orchid, Current Biology (2020), https://doi.org/10.1016/j.cub.2020.10.024

analyzed pentane extracts of flowers by using gas chromatography coupled with mass spectrometry (GCMS), to identify the presence of diacetin.[8,36] This volatile acetylated glycerol is thought to be a derivative of the biosynthesis of fatty floral oil, and is considered a universal cue for oil-collecting bees, including *R. neliana*, the pollinator of the *BEE* form.[8] Consistent with the results from staining, GCMS analyses confirmed the presence of diacetin and also triacetin in all six forms (Figure 2). However, quantities were much higher in flowers of the *BEE* form than in the *MOTH* forms (diacetin: $\chi^2 = 113.52$, $p < 0.001$, bee: moth production ratio = 7.83; triacetin: $\chi^2 = 25.731$, $p < 0.001$, ratio = 11.46) (Figure 2). The dependence of *R. neliana* antennal responses on diacetin concentration[8] might explain why bees only visit the *BEE* form of *S. longicauda*. Analyses of floral extracts further revealed the unique presence in the *BEE* form of 2-tridecanone (Figure 2), which is known to trigger antennal responses in oil-collecting bees.[8] Presence of 2-tridecanone is unknown from moth-pollinated *Satyrium* species,[29] but has been reported from the only other—distantly related—*Satyrium* species that is pollinated by oil-collecting bees.[37,38]

To further characterize traits involved in pollinator attraction and morphological fit between flower and pollinator, we quantified color, morphology, and floral headspace volatiles across the six forms. Analysis of spectral reflectance of flowers in a bee vision model showed strong overlap among several *MOTH* forms, but also between the *BEE* form and two *MOTH* forms (Figure 2). A multivariate analysis of 12 quantitative morphometric traits showed that although plants cluster by form (PERMANOVA: $f = 127.36$, $p < 0.001$), there are no clear discontinuities among forms (Figure 2). Furthermore, the mean Euclidean morphological distance between *BEE* and *MOTH* forms was similar to that among *MOTH* forms ($\chi^2 = 0.334$, $p = 0.56$).

Analysis of floral scent headspace sampled during day and night revealed that time of day, form, and the interaction between these factors all differed significantly (2-way PERMANOVA: time of day $f = 45.646$, $p < 0.001$; form $f = 13.556$, $p < 0.001$; time of day × form $f = 6.0347$, $p < 0.001$) (Figure 2). However, similar to the results for morphometric characters, Bray-Curtis similarity of headspace for *BEE* and *MOTH* form comparisons were similar to those among *MOTH* forms, both during day and night (day: $\chi^2 = 0.095$, $p = 0.76$; night: $\chi^2 = 2.64$, $p = 0.10$) (Figure 2; Table S3). A similarity percentage analysis showed that scent across all forms was dominated by aromatic compounds, in particular (E)-cinnamyl alcohol, and that the compounds that dominate the *MOTH* forms also dominate the *BEE* form (Table S3). Several aromatic compounds in the *S. longicauda* headspace are known to elicit antennal responses in the hawkmoth pollinator *B. schenki*.[36]

Given the overall similarity in flower shape, color, and headspace scent, we predicted that the lack of nocturnal moth visitation to the *BEE* form could reflect the lack of a suitable reward. Measurements of nectar volume and sugar concentration confirmed an almost complete absence of nectar in the floral spurs of the *BEE* form, whereas in the *MOTH* forms, nectar volume per flower ranged between 0.5–2.5 μl, resulting in a total sugar availability per flower of 0.2–0.8 mg (Figure 2).

In flowers of the *BEE* form, the near-absence of nectar and the apparent collection of oil by bees from the labellum galea suggest that floral spurs might no longer have a function for pollination. Some oil-producing plants in South Africa produce oil in floral spurs,[39] but the length of their spurs usually closely matches the foreleg length of the pollinating *Rediviva* bees.[40,41] In contrast, the distance from spur tips to the rostellum of the *BEE* form is much longer than the foreleg of local *R. neliana* (mean ± SD functional spur length = 24.00 ± 2.18 mm, n = 50; mean ± SD foreleg length of *R. neliana* females = 10.68 ± 0.58 mm, n = 13), but within the range for moth-pollinated *Satyrium* species (10–24.5 mm), whereas spurs of other bee-pollinated *Satyrium* species are typically shorter (range 5–11.5 mm).[17] Furthermore, the floral spurs of the *BEE* form are much narrower than those of *Diascia* flowers and the only other *Satyrium* species pollinated by oil-collecting bees[38] and thus likely too narrow to accommodate the broad pilose forelegs of *Rediviva* females. In contrast, tongue insertion by moths during nectar foraging indicates a clear function for spurs that is likely to result in strong selection for optimal nectar spur lengths in the *MOTH* forms.[25,42–44] Coefficients of variation (CVAs) for spur length are significantly larger in the *BEE* than in the *MOTH* forms (CVA *BEE* = 11.22; mean ± SD CVA *MOTH* = 7.35 ± 0.73; modified signed-likelihood ratio test (SLRT) statistic = 20.4, $p = 0.0011$), but not for lateral sepal length (CVA *BEE* = 9.25; mean ± SD CVA *MOTH* = 8.56 ± 0.86; SLRT statistic = 4.83, $p = 0.44$), consistent with contrasting signatures of relaxed and strong selection on floral spurs but not other floral traits in *BEE* and *MOTH* forms, respectively (cf. Evans and Bernard[45] and Fenster[46]). The presence, in the population of the *BEE* form, of a mutant that almost completely lacked floral spurs (Figure 1) further suggested relaxed selection on spur length in the *BEE* form. Finally, experimental shortening of floral spurs of the *BEE* and a *MOTH* form confirmed that both pollinarium removal (male fitness component) and massulae deposition on stigmas (female fitness component) were significantly reduced by this manipulation in the *MOTH*, but not the *BEE* form (Figure 3) (cf. Nilsson[42]).

Evolution of Pollination Systems and Floral Traits

Floral traits that do not differ among pollination systems likely did not evolve in association with a pollinator shift. Evolution of such traits might precede a pollinator shift and indicate a pre-adaptation or might represent vestigial structures that have not yet been

(C) Linear discriminant analysis of 12 morphological traits shows that the morphology of the *BEE* form does on average not differ more from *MOTH* forms than *MOTH* forms differ among one another.

(D) Non-metric multidimensional scaling analysis of floral scent profiles for all forms suggests that the overall scent profile of the *BEE* form is similar to that of the *MOTH* forms. Circles and squares indicate day and night samples respectively.

(E–G) Shown in (E) is mean ± SE nectar volume per flower, in (F) mean ± SE total sugar production per flower, and in (G) mean ± SE spur length (tip to point of fusion with labellum). These three traits all differ significantly among forms (nectar volume: $\chi^2 = 442.09$, $p < 0.001$; sugar content $\chi^2 = 399.51$, $p < 0.001$; spur length: $\chi^2 = 2338.10$, $p < 0.001$).

Letters indicate which forms differ significantly from each other ($p < 0.01$). The legend at the bottom right applies to (B)–(G). See also Figure S2 and Table S3.

Please cite this article in press as: Castañeda-Zárate et al., Food Reward Chemistry Explains a Novel Pollinator Shift and Vestigialization of Long Floral Spurs in an Orchid, Current Biology (2020), https://doi.org/10.1016/j.cub.2020.10.024

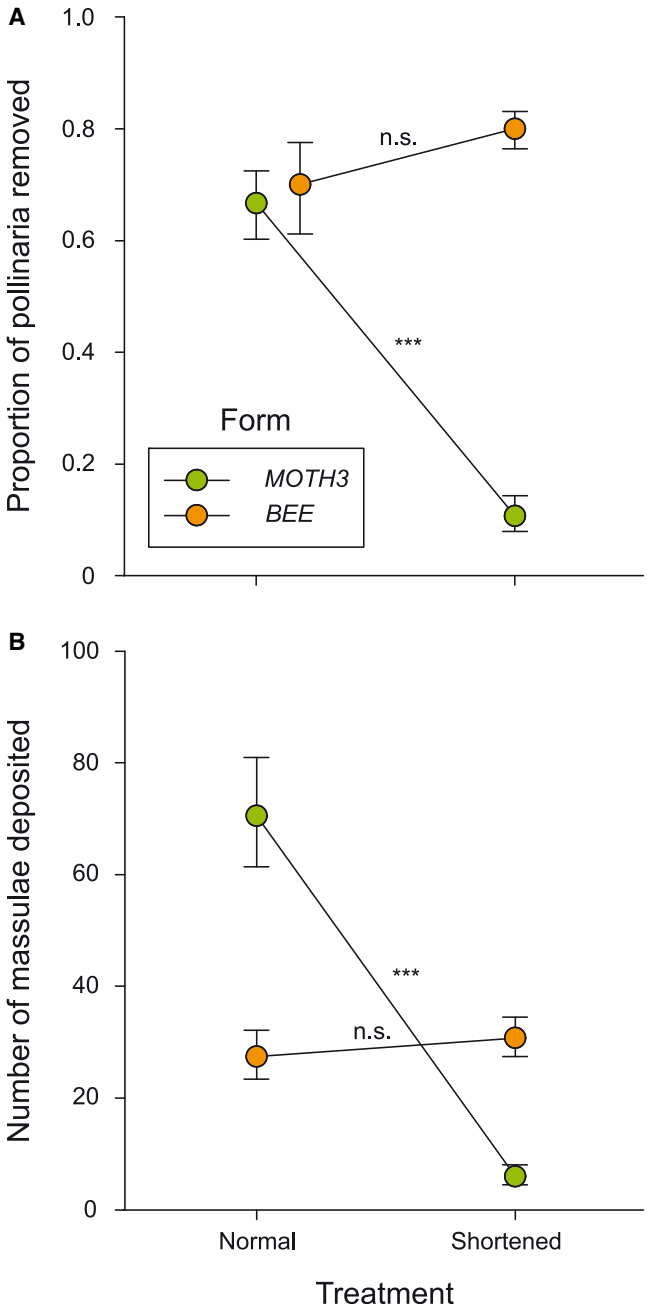

Figure 3. Effect of Spur Shortening on Male and Female Fitness of Two Forms of *Satyrium longicauda* with Contrasting Pollination Systems

Shown in (A) is the mean ± SE proportion of flowers with pollinaria removed (form × treatment: $\chi^2 = 29.83$; $p < 0.001$) and (B) mean ± SE number of massulae deposited on the stigma (form × treatment: $\chi^2 = 50.83$, $p < 0.001$) of the *BEE* and a *MOTH* form. ***$p < 0.001$, n.s., not significant.

lost. To distinguish between these possibilities, we implemented a phylogenetic framework (cf. van der Niet and Johnson[1] and Coddington[47]). A phylogenetic tree based on Bayesian analysis of nuclear DNA sequences of multiple individuals per form supported monophyly of each form, with the exception of *MOTH4*, which was an unresolved polytomy (Figure S3). Together with the morphological clustering of sympatric forms (Figure 2), this suggests that each form represents an independent evolutionary lineage and justifies the application of a phylogenetic approach. The phylogenetic tree based on plastid DNA sequences was less resolved and supported, and partly incongruent with the results from the nuclear data, but also unambiguously supported a sister relationship between the *BEE* and *MOTH1* form (Figure S3).

Ancestral character state reconstruction using parsimony on topologies reconstructed from nuclear and plastid data both showed that pollination by oil-collecting bees in the *BEE* form is derived from moth-pollination in *S. longicauda* (Figure 4). This result was supported by likelihood-based optimization for the nuclear and plastid datasets (Figure S4). Although shifts away from oil production are relatively well-studied,[10,48,49] understanding of the evolutionary origin of pollination by oil-collecting bees was hitherto limited to quantification of the temporal accumulation of lineages and of frequent independent evolution.[49] Previous work on the origin of oil flowers suggested that these might have originated from bee-pollinated ancestors in which pollen and/or nectar was the main reward.[50,51] Some bee-pollinated species jointly produce nectar and oil,[51,52] suggesting a transition through an intermediate stage of double function (cf. Stebbins[13]). Our results thus reveal a novel route for the evolution of pollination by oil-collecting bees.

We propose that the evolution of reward chemistry was key to this unusual transition from moth to bee pollination. The clearly derived nature of bee pollination in this system, combined with the presence of lipids and diacetin in all six forms, suggests that these compounds did not evolve *de novo* in association with the shift to bee pollination. A broader analysis revealed that apart from a record of pollination by oil-collecting *Rediviva* bees in a distantly related *Satyrium* species,[38] no traces of diacetin were found in a sample of *Satyrium* species that includes representatives of all major lineages in the genus.[53] Ancestral character state reconstruction using the topology based on nuclear data suggests that production of detectable amounts of diacetin evolved in the common ancestor of *S. longicauda* (Figure 4). The results based on plastid data suggest the gain of diacetin at the root of the genus with two losses, but this is likely an artifact because of the sparse sampling of species for diacetin in the large clade to which *S. longicauda* belongs[53] (Figure 4). Nevertheless, plastid results and likelihood-based results all imply ancestral presence of diacetin in *S. longicauda* (Figure S4). Diacetin presence in the moth-pollinated forms might have served as a pre-adaptation that triggered occasional visitation by oil-collecting bees (cf. Manning and Goldblatt[51]), followed by additional upregulation and production of 2-tridecanone in response to selection by oil-collecting bees.[8] Presence of diacetin has been reported for another moth-pollinated orchid in a study that also found that moth antennae respond to it.[36] More research is needed to understand the presence of diacetin in species that are not bee pollinated, in order to clarify whether it is a legacy of ancestral pollination by oil-collecting bees or has a functional role in these species.

The shift from moth to bee pollination is associated with a small but significant decrease in spur length (Figure 2). This trend is a departure from the expected unidirectional trajectory of increased spur length evolution[54,55] but could be explained by the vestigialization of floral spurs associated with the shift from

Please cite this article in press as: Castañeda-Zárate et al., Food Reward Chemistry Explains a Novel Pollinator Shift and Vestigialization of Long Floral Spurs in an Orchid, Current Biology (2020), https://doi.org/10.1016/j.cub.2020.10.024

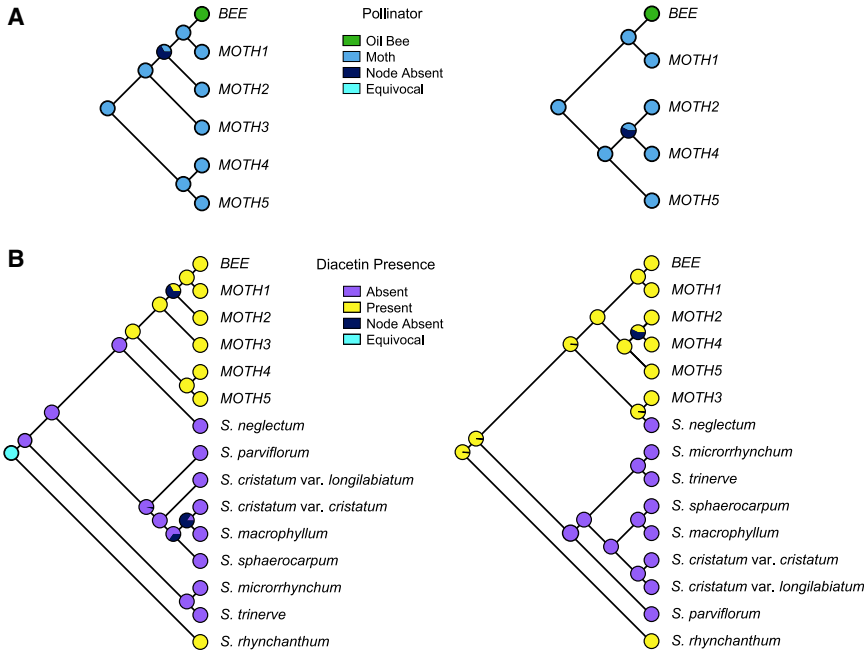

Figure 4. Ancestral Character State Reconstruction

(A) Pollinator (*Satyrium longicauda* complex only). (B) Diacetin (*Satyrium*).

Results are obtained by using parsimony reconstruction and mapped onto a randomly chosen tree from Bayesian inference of nuclear (left) and plastid (right) DNA sequences. See also Figures S3 and S4.

nectar-foraging moth pollination to oil-collecting bee pollination.[56]

The sympatric ecotypes in *S. longicauda* might represent early stages of speciation, determined by ethological isolation.[57] The existence of multiple moth-pollinated lineages and a single derived *BEE* form would render this a case of progenitor-derivative speciation.[58] Given that the *BEE* form is currently only known from a single site, where it co-occurs with its closest moth-pollinated relatives, the possibility of sympatric speciation cannot be rejected.[59,60] However, in contrast to oceanic islands where historical sympatry is more likely to have been maintained over geological time scales,[60] initial evolution in allopatry, followed by range extension and extinction remains a possibility in this case.[61] Furthermore, the role of additional isolating factors, such as micro-habitat differences, phenological shifts, and post-zygotic isolation need to be investigated to fully understand the strength, nature, and sequence of evolution of reproductive isolation.[62–64]

CONCLUSION

Pollinator shifts have been important for driving extant floral diversity, but the relatively discontinuous nature of suites of floral traits in the currently observable end points of evolution make reconstruction of the underlying evolutionary process challenging. Our study demonstrates the significance of minor modifications in floral chemistry for the initiation of major shifts between insect pollinators belonging to different orders. A similarly pivotal role for minor modifications of floral chemistry has previously been shown in sexually deceptive pollination systems, but these typically involve shifts between closely related pollinators belonging to the same order or even genus.[65–67]

The similarity in floral traits among ecotypes of *S. longicauda* with very different pollination systems, suggests that broadly defined floral syndromes can be inadequate for predicting pollinators, especially if not all traits are functional. Floral spurs in particular are considered a key innovation for angiosperm diversification[68] and their adaptive nature has been emphasized in many studies,[54,55,69] often through covariation between plant and pollinator traits.[70] Our study demonstrates a mismatch between floral spurs and pollinators and indicates that floral spurs can be vestigial. Although vestigialization in plants is well-known from transitions from outcrossing to selfing,[71–73] few studies have combined phylogenetic and experimental approaches to provide evidence for vestigialization during pollinator shifts in entirely pollinator-dependent plants.[10] Our study improves understanding of the sequence of evolution of trait syndromes by providing an example of how divergence in floral rewards could precede that of morphological traits, resulting in a stage of transition characterized by trait vestigialization.

STAR★METHODS

Detailed methods are provided in the online version of this paper and include the following:

- KEY RESOURCES TABLE
- RESOURCE AVAILABILITY
  - Lead Contact
  - Materials Availability
  - Data and Code Availability
- EXPERIMENTAL MODEL AND SUBJECT DETAILS
  - Study species and site
- METHOD DETAILS
  - Pollination ecology
  - Quantification of floral traits
  - Phylogenetic inference
- QUANTIFICATION AND STATISTICAL ANALYSIS

- Timing of pollination
- Floral trait quantification
- Phylogenetic analyses and ancestral character state reconstruction

SUPPLEMENTAL INFORMATION

Supplemental Information can be found online at https://doi.org/10.1016/j.cub.2020.10.024.

ACKNOWLEDGMENTS

We thank Ruth Cozien for comments on a draft of the manuscript. S.D.J. was supported by a grant from the National Research Foundation of South Africa (46372). M.C.Z. was supported by a scholarship from The World Academy of Sciences (TWAS) through the National Research Foundation of South Africa (SFH160623173837). T.N. was supported by incentive funding from the National Research Foundation of South Africa (109547). We thank Ezemvelo KZN Wildlife for research permits. We thank Mondi for allowing access to the Mount Gilboa reserve. Carmen Demmer, Ruth Cozien, and Daichi Funamoto are thanked for help with fieldwork. We thank Stefan Dötterl for providing the Kovats Retention Indices of acytelated glycerols. We thank Kim Steiner and Denis Brothers for help with the identification of bee species. Sergio Ramos is thanked for his help in editing the graphical abstract.

AUTHOR CONTRIBUTIONS

Conceptualization, T.N. and S.D.J; Methodology, T.N., S.D.J., and M.C.Z.; Formal Analysis, M.C.Z, S.D.J., and T.N. jointly analyzed the data; Investigation, M.C.Z.; Resources, S.D.J. and T.N.; Writing, M.C.Z, S.D.J., and T.N jointly wrote the manuscript; Visualization, M.C.Z, T.N., and S.D.J.; Supervision, T.N. and S.D.J.; Project Administration, T.N., S.D.J., and M.C.Z.; Funding Acquisition, S.D.J., M.C.Z., and T.N.

DECLARATION OF INTERESTS

The authors declare no competing interests.

Received: June 15, 2020
Revised: October 2, 2020
Accepted: October 8, 2020
Published: November 5, 2020

REFERENCES

1. van der Niet, T., and Johnson, S.D. (2012). Phylogenetic evidence for pollinator-driven diversification of angiosperms. Trends Ecol. Evol. *27*, 353–361.
2. Hernández-Hernández, T., and Wiens, J.J. (2020). Why are there so many flowering plants? A multiscale analysis of plant diversification. Am. Nat. *195*, 948–963.
3. Gervasi, D.D.L., and Schiestl, F.P. (2017). Real-time divergent evolution in plants driven by pollinators. Nat. Commun. *8*, 14691.
4. Armbruster, W.S., and Muchhala, N. (2009). Associations between floral specialization and species diversity: cause, effect, or correlation? Evol. Ecol. *23*, 159–179.
5. van der Niet, T., Peakall, R., and Johnson, S.D. (2014). Pollinator-driven ecological speciation in plants: new evidence and future perspectives. Ann. Bot. *113*, 199–211.
6. Phillips, R.D., Peakall, R., van der Niet, T., and Johnson, S.D. (2020). Niche perspectives on plant-pollinator interactions. Trends Plant Sci. *25*, 779–793.
7. Kay, K.M., and Sargent, R.D. (2009). The role of animal pollination in plant speciation: Integrating ecology, geography, and genetics. Annu. Rev. Ecol. Evol. Syst. *40*, 637–656.
8. Schaffler, I., Steiner, K.E., Haid, M., van Berkel, S.S., Gerlach, G., Johnson, S.D., Wessjohann, L., and Dotterl, S. (2015). Diacetin, a reliable cue and private communication channel in a specialized pollination system. Sci. Rep. *5*, 11.
9. Armbruster, W.S., Pélabon, C., Hansen, T.F., and Bolstad, G.H. (2009). Macroevolutionary patterns of pollination accuracy: a comparison of three genera. New Phytol. *183*, 600–617.
10. Steiner, K. (1998). The evolution of beetle pollination in a South African orchid. Am. J. Bot. *85*, 1180–1193.
11. Fong, D.W., Kane, T.C., and Culver, D.C. (1995). Vestigialization and loss of nonfunctional characters. Annu. Rev. Ecol. Syst. *26*, 249–268.
12. Lahti, D.C., Johnson, N.A., Ajie, B.C., Otto, S.P., Hendry, A.P., Blumstein, D.T., Coss, R.G., Donohue, K., and Foster, S.A. (2009). Relaxed selection in the wild. Trends Ecol. Evol. *24*, 487–496.
13. Stebbins, G.L. (1970). Adaptive radiation of reproductive characteristics in angiosperms. I. Pollination mechanisms. Annu. Rev. Ecol. Syst. *1*, 307–326.
14. Grant, V., and Grant, K.A. (1965). Flower pollination in the *Phlox* family (New York: Columbia University Press).
15. Armbruster, W.S. (1985). Patterns of character divergence and the evolution of reproductive ecotypes of *Dalechampia scandens* (Euphorbiaceae). Evolution *39*, 733–752.
16. Johnson, S.D. (2006). Pollinator-driven speciation in plants. In The ecology and evolution of flowers, L.D. Harder, and S.C.H. Barrett, eds. (Oxford: Oxford University Press), pp. 295–310.
17. Hall, A.V. (1982). A revision of the southern African species of *Satyrium*. Contr. Bolus Herb. *10*, 1–142.
18. Turesson, G. (1922). The genotypical response of the plant species to the habitat. Hereditas *3*, 211–350.
19. Armbruster, W.S. (2014). Floral specialization and angiosperm diversity: phenotypic divergence, fitness trade-offs and realized pollination accuracy. AoB Plants *6*, 24.
20. Eckert, C.G. (2002). Effect of geographical variation in pollinator fauna on the mating system of *Decodon verticillatus* (Lythraceae). Int. J. Plant Sci. *163*, 123–132.
21. Johnson, S.D., Harris, L.F., and Proches, S. (2009). Pollination and breeding systems of selected wildflowers in a southern African grassland community. S. Afr. J. Bot. *75*, 630–645.
22. Johnson, S.D., Peter, C.I., Ellis, A.G., Boberg, E., Botes, C., and van der Niet, T. (2011). Diverse pollination systems of the twin-spurred orchid genus *Satyrium* in African grasslands. Plant Syst. Evol. *292*, 95–103.
23. van der Niet, T., Liltved, W.R., and Johnson, S.D. (2011). More than meets the eye: a morphological and phylogenetic comparison of long-spurred, white-flowered *Satyrium* species (Orchidaceae) in South Africa. Bot. J. Linn. Soc. *166*, 417–430.
24. Vogel, S. (1954). Blütenbiologische Typen als Elemente der Sippengliederug, dargestellt anhand der Flora Südafrikas (Jena: Fischer).
25. Johnson, S.D., Moré, M., Amorim, F.W., Haber, W.A., Frankie, G.W., Stanley, D.A., Coccuci, A.A., and Raguso, R.A. (2017). The long and the short of it: a global analysis of hawkmoth pollination niches and interaction networks. Funct. Ecol. *31*, 101–115.
26. Johnson, S.D., Balducci, M.G., Bijl, A., Castañeda-Zárate, M., Cozien, R.J., Ortmann, C.R., and Van der Niet, T. (2020). From dusk till dawn: camera traps reveal the diel patterns of flower feeding by hawkmoths. Ecol. Entomol. *45*, 751–755.
27. Pauw, A. (2006). Floral syndromes accurately predict pollination by a specialized oil-collecting bee *(Rediviva peringueyi*, Melittidae) in a guild of South African orchids (Coryciinae). Am. J. Bot. *93*, 917–926.
28. Waterman, R.J., Bidartondo, M.I., Stofberg, J., Combs, J.K., Gebauer, G., Savolainen, V., Barraclough, T.G., and Pauw, A. (2011). The effects of above- and belowground mutualisms on orchid speciation and coexistence. Am. Nat. *177*, E54–E68.

29. van der Niet, T., Jürgens, A., and Johnson, S.D. (2015). Is the timing of scent emission correlated with insect visitor activity and pollination in long-spurred *Satyrium* species? Plant Biol (Stuttg) *17*, 226–237.
30. Vogel, S. (1984). The *Diascia* flower and its bee - an oil-based symbiosis in southern Africa. Acta Bot. Neerl. *33*, 509–518.
31. Manning, J.C., and Brothers, D.J. (1986). Floral relations of four species of *Rediviva* in Natal. J. Entomol. Soc. South. Afr. *49*, 107–114.
32. Whitehead, V.B. (1984). The bee *Redviva longimanus* Michener (Apoideae: Melittidae), collecting pollen and oil from *Diascia longicornis* (Thumb.) Druce (Schrophulariaceae). S. Afr. J. Sci. *80*, 286.
33. Kuhlmann, M., and Hollens, H. (2015). Morphology of oil-collecting pilosity of female *Rediviva* bees (Hymenoptera: Apoidea: Melittidae) reflects host plant use. J. Nat. Hist. *49*, 561–573.
34. Dumri, K., Seipold, L., Schmidt, J., Gerlach, G., Dötterl, S., Ellis, A.G., and Wessjohann, L.A. (2008). Non-volatile floral oils of *Diascia* spp. (Scrophulariaceae). Phytochemistry *69*, 1372–1383.
35. Buchmann, S.L. (1987). The ecology of oil flowers and their bees. Annu. Rev. Ecol. Syst. *18*, 343–369.
36. Johnson, S.D., Balducci, M.G., and Shuttleworth, A. (2020). Hawkmoth pollination of the orchid *Habenaria clavata*: mechanical wing guides, floral scent and electroantennography. Biol. J. Linn. Soc. Lond. *129*, 213–226.
37. Steiner, K.E., Kaiser, R., and Dötterl, S. (2011). Strong phylogenetic effects on floral scent variation of oil-secreting orchids in South Africa. Am. J. Bot. *98*, 1663–1679.
38. Whitehead, V.B., and Steiner, K.E. (2001). Oil-collecting bees of the winter rainfall area of South Africa (Melittidae, *Rediviva*). Ann. S. Afr. Mus. *108*, 143–277.
39. Hollens, H., van der Niet, T., Cozien, R., and Kuhlmann, M. (2017). A spurious inference: Pollination is not more specialized in long-spurred than in spurless species in *Diascia-Rediviva* mutualisms. Flora *232*, 73–82.
40. Steiner, K.E., and Whitehead, V.B. (1990). Pollinator adaptation to oil-secreting flowers - *Redivivia* and *Diascia*. Evolution *44*, 1701–1707.
41. Pauw, A., Kahnt, B., Kuhlmann, M., Michez, D., Montgomery, G.A., Murray, E., and Danforth, B.N. (2017). Long-legged bees make adaptive leaps: linking adaptation to coevolution in a plant-pollinator network. Proc. Biol. Sci. *284*, 7.
42. Nilsson, L.A. (1988). The evolution of flowers with deep corolla tubes. Nature *334*, 147–149.
43. Anderson, B., Alexandersson, R., and Johnson, S.D. (2010). Evolution and coexistence of pollination ecotypes in an African *Gladiolus* (Iridaceae). Evolution *64*, 960–972.
44. Trunschke, J., Sletvold, N., and Ågren, J. (2020). Manipulation of trait expression and pollination regime reveals the adaptive significance of spur length. Evolution *74*, 597–609.
45. Evans, M.R., and Barnard, P. (1995). Variable sexual ornaments in Scarlet-tufted Malachite sunbirds (*Nectarinia johnstoni*) on Mount Kenya. Biol. J. Linn. Soc. Lond. *54*, 371–381.
46. Fenster, C.B. (1991). Selection on floral morphology by hummingbirds. Biotropica *23*, 98–101.
47. Coddington, J.A. (1988). Cladistic tests of adaptional hypotheses. Cladistics *4*, 3–22.
48. Davis, C.C., Schaefer, H., Xi, Z., Baum, D.A., Donoghue, M.J., and Harmon, L.J. (2014). Long-term morphological stasis maintained by a plant-pollinator mutualism. Proc. Natl. Acad. Sci. USA *111*, 5914–5919.
49. Renner, S.S., and Schaefer, H. (2010). The evolution and loss of oil-offering flowers: new insights from dated phylogenies for angiosperms and bees. Philos. Trans. R. Soc. Lond. B Biol. Sci. *365*, 423–435.
50. Martins, A.C., Scherz, M.D., and Renner, S.S. (2014). Several origins of floral oil in the Angelonieae, a southern hemisphere disjunct clade of Plantaginaceae. Am. J. Bot. *101*, 2113–2120.
51. Manning, J.C., and Goldblatt, P. (2005). Radiation of pollination systems in the Cape genus *Tritoniopsis* (Iridaceae: Crocoideae) and the development of bimodal pollination strategies. Int. J. Plant Sci. *166*, 459–474.
52. Ferreiro, G., Baranzelli, M.C., Sersic, A.N., and Cocucci, A.A. (2017). Patterns of phenotypic selection for oil and nectar in *Monttea aphylla* (Plantaginaceae) in a geographic mosaic of interactions with pollinators. Flora *232*, 47–55.
53. van der Niet, T., Linder, H.P., Bytebier, B., and Bellstedt, D.U. (2005). Molecular markers reject monophyly of the subgenera of *Satyrium* (Orchidaceae). Syst. Bot. *30*, 263–274.
54. Whittall, J.B., and Hodges, S.A. (2007). Pollinator shifts drive increasingly long nectar spurs in columbine flowers. Nature *447*, 706–709.
55. Pauw, A., Stofberg, J., and Waterman, R.J. (2009). Flies and flowers in Darwin's race. Evolution *63*, 268–279.
56. Ellis, A.G., and Johnson, S.D. (2010). Gender differences in the effects of floral spur length manipulation on fitness in a hermaphrodite orchid. Int. J. Plant Sci. *171*, 1010–1019.
57. Grant, V. (1994). Modes and origins of mechanical and ethological isolation in angiosperms. Proc. Natl. Acad. Sci. USA *91*, 3–10.
58. Schlüter, P.M., Ruas, P.M., Kohl, G., Ruas, C.F., Stuessy, T.F., and Paulus, H.F. (2011). Evidence for progenitor-derivative speciation in sexually deceptive orchids. Ann. Bot. *108*, 895–906.
59. Peakall, R., and Whitehead, M.R. (2014). Floral odour chemistry defines species boundaries and underpins strong reproductive isolation in sexually deceptive orchids. Ann. Bot. *113*, 341–355.
60. Savolainen, V., Anstett, M.C., Lexer, C., Hutton, I., Clarkson, J.J., Norup, M.V., Powell, M.P., Springate, D., Salamin, N., and Baker, W.J. (2006). Sympatric speciation in palms on an oceanic island. Nature *441*, 210–213.
61. Losos, J.B., and Glor, R.E. (2003). Phylogenetic comparative methods and the geography of speciation. Trends Ecol. Evol. *18*, 220–227.
62. Schemske, D.W. (2010). Adaptation and the origin of species. Am. Nat. *176* (*Suppl 1*), S4–S25.
63. Ramsey, J., Bradshaw, H.D., Jr., and Schemske, D.W. (2003). Components of reproductive isolation between the monkeyflowers *Mimulus lewisii* and *M. cardinalis* (Phrymaceae). Evolution *57*, 1520–1534.
64. Lowry, D.B., Modliszewski, J.L., Wright, K.M., Wu, C.A., and Willis, J.H. (2008). The strength and genetic basis of reproductive isolating barriers in flowering plants. Philos. Trans. R. Soc. B Biol. Sci. *363*, 3009–3021.
65. Peakall, R., Ebert, D., Poldy, J., Barrow, R.A., Francke, W., Bower, C.C., and Schiestl, F.P. (2010). Pollinator specificity, floral odour chemistry and the phylogeny of Australian sexually deceptive *Chiloglottis* orchids: implications for pollinator-driven speciation. New Phytol. *188*, 437–450.
66. Schlüter, P.M., Xu, S., Gagliardini, V., Whittle, E., Shanklin, J., Grossniklaus, U., and Schiestl, F.P. (2011). Stearoyl-acyl carrier protein desaturases are associated with floral isolation in sexually deceptive orchids. Proc. Natl. Acad. Sci. USA *108*, 5696–5701.
67. Vereecken, N.J., Wilson, C.A., Hötling, S., Schulz, S., Banketov, S.A., and Mardulyn, P. (2012). Pre-adaptations and the evolution of pollination by sexual deception: Cope's rule of specialization revisited. Proc. Biol. Sci. *279*, 4786–4794.
68. Hodges, S.A., and Arnold, M.L. (1995). Spurring plant diversification: are floral nectar spurs a key innovation? Proc. R. Soc. Lond. B Biol. Sci. *262*, 343–348.
69. Johnson, S.D., and Steiner, K.E. (1997). Long-tongued fly pollination and evolution of floral spur length in the *Disa draconis* complex (Orchidaceae). Evolution *51*, 45–53.
70. Anderson, B., and Johnson, S.D. (2009). Geographical covariation and local convergence of flower depth in a guild of fly-pollinated plants. New Phytol. *182*, 533–540.
71. Button, L., Villalobos, A.L., Dart, S.R., and Eckert, C.G. (2012). Reduced petal size and color associated with transitions from outcrossing to selfing in *Camissoniopsis cheieranthifoloia* (Onagraceae). Int. J. Plant Sci. *173*, 251–260.

72. Dorken, M.E., Neville, K.J., and Eckert, C.G. (2004). Evolutionary vestigialization of sex in a clonal plant: selection versus neutral mutation in geographically peripheral populations. Proc. Biol. Sci. *271*, 2375–2380.
73. Doubleday, L.A.D., Raguso, R.A., and Eckert, C.G. (2013). Dramatic vestigialization of floral fragrance across a transition from outcrossing to selfing in *Abronia umbellata* (Nyctaginaceae). Am. J. Bot. *100*, 2280–2292.
74. Kearse, M., Moir, R., Wilson, A., Stones-Havas, S., Cheung, M., Sturrock, S., Buxton, S., Cooper, A., Markowitz, S., Duran, C., et al. (2012). Geneious Basic: an integrated and extendable desktop software platform for the organization and analysis of sequence data. Bioinformatics *28*, 1647–1649.
75. Maddison, W.P., and Maddison, D.R. (2019). Mesquite: A modular system for evolutionary analysis. www.mesquiteproject.org.
76. Ronquist, F., Teslenko, M., van der Mark, P., Ayres, D.L., Darling, A., Höhna, S., Larget, B., Liu, L., Suchard, M.A., and Huelsenbeck, J.P. (2012). MrBayes 3.2: efficient Bayesian phylogenetic inference and model choice across a large model space. Syst. Biol. *61*, 539–542.
77. Stein, S., Mirokhin, Y., Tchekhovskoi, D., and Mallard, G. (2011). The NIST Mass Spectral Search Program for the NIST/EPA/NIH Spectral Library Version 2.0 g (The Standard Reference Data Program of the National Institute of Standards and Technology).
78. Hammer, Ø., Harper, D.A.T., and Ryan, P.D. (2001). PAST: Paleontological statistics software package for education and data analysis. Palaeontol. Electronica *4*, 1–9.
79. Clark, K.R., and Gorley, R.N. (2006). Primer v6: User Manual/Tutorial (Plymouth: Primer-E).
80. Team, R. (2020). RStudio: Integrated Development for R. *http://www.rstudio.com/*.
81. Venables, W.N., and Ripley, B.D. (2002). Modern applied statistics with S, Fourth Edition (New York: Springer).
82. Krishnamoorthy, K., and Lee, M. (2014). Improved tests for the equality of normal coefficients of variation. Comput. Stat. *29*, 215–232.
83. Maia, R., Eliason, C.M., Bitton, P.P., Doucet, S.M., and Shawkey, M.D. (2013). pavo: an R package for the analysis, visualization and organization of spectral data. Methods Ecol. Evol. *4*, 906–913.
84. Goloboff, P.A., and Catalano, S.A. (2016). TNT version 1.5, including a full implementation of phylogenetic morphometrics. Cladistics *32*, 221–238.
85. Rambaut, A., Drummond, A.J., Xie, D., Baele, G., and Suchard, M.A. (2018). Posterior Summarization in Bayesian Phylogenetics Using Tracer 1.7. Syst. Biol. *67*, 901–904.
86. Pinhey, E.C.G. (1975). Moths of Southern Africa (Cape Town: Tafelberg Publishers Ltd).
87. Dafni, A. (1992). Pollination Biology: A Practical Approach (Oxford: Oxford University Press).
88. Johnson, S.D. (1997). Insect pollination and floral mechanisms in South African species of *Satyrium* (Orchidaceae). Plant Syst. Evol. *204*, 195–206.
89. Johnson, S.D. (1997). Pollination ecotypes of *Satyrium hallackii* (Orchidaceae) in South Africa. Bot. J. Linn. Soc. *123*, 225–235.
90. Botes, C., van der Niet, T., Cowling, R.M., and Johnson, S.D. Is biodiversity underestimated by classical herbarium-based taxonomy? A multidisciplinary case study in *Satyrium* (Orchidaceae). Bot. J. Linn. Soc., in press.
91. van der Niet, T., and Peter Linder, H. (2008). Dealing with incongruence in the quest for the species tree: a case study from the orchid genus *Satyrium*. Mol. Phylogenet. Evol. *47*, 154–174.
92. Bateman, R.M., Hollingsworth, P.M., Preston, J., Yi-Bo, L., Pridgeon, A.M., and Chase, M.W. (2003). Molecular phylogenetics and evolution of Orchidinae and selected Habenariinae (Orchidaceae). Bot. J. Linn. Soc. *142*, 1–40.
93. Shaw, J., Lickey, E.B., Schilling, E.E., and Small, R.L. (2007). Comparison of whole chloroplast genome sequences to choose noncoding regions for phylogenetic studies in angiosperms: the tortoise and the hare III. Am. J. Bot. *94*, 275–288.
94. White, T.J., Bruns, T., Lee, S., and Taylor, J. (1990). Amplification and direct sequencing of fungal ribosomal RNA genes for phylogenetics. In PCR protocols: a guide to methods and applications, M.A. Innis, D.H. Gelfand, J.J. Sninsky, and T.J. White, eds. (San Diego, California: Academic Press), pp. 315–324.
95. Taberlet, P., Gielly, L., Pautou, G., and Bouvet, J. (1991). Universal primers for amplification of three non-coding regions of chloroplast DNA. Plant Mol. Biol. *17*, 1105–1109.
96. Kocyan, A., Qiu, Y.L., Endress, P.K., and Conti, E. (2004). A phylogenetic analysis of Apostasioideae (Orchidaceae) based on ITS, trnL-F and matK sequences. Plant Syst. Evol. *247*, 203–213.
97. Šidák, Z. (1967). Rectangular confidence regions for the means of multivariate normal distributions. J. Am. Stat. Assoc. *62*, 626–633.
98. Chittka, L. (1992). The colour hexagon: a chromaticity diagram based on photoreceptor excitations as a general representation of colour opponency. J. Comp. Physiol. A Neuroethol. Sens. Neural Behav. Physiol. *170*, 533–543.
99. Peitsch, D., Fietz, A., Hertel, H., de Souza, J., Ventura, D.F., and Menzel, R. (1992). The spectral input systems of hymenopteran insects and their receptor-based colour vision. J. Comp. Physiol. A Neuroethol. Sens. Neural Behav. Physiol. *170*, 23–40.
100. Amirav, A., and Dagan, S. (1997). A direct sample introduction device for mass spectrometry studies and gas chromatography mass spectrometry analyses. Eur. Mass Spectrom. *3*, 105–111.
101. Marwick, B., and Krishnamoorthy, K. (2019). cvequality: Tests for the Equality of Coefficients of Variation from Multiple Groups. R software package version 0.1.3. https://github.com/benmarwick/cvequality.
102. Felsenstein, J. (1985). Confidence limits on phylogenies - an approach using the bootstrap. Evolution *39*, 783–791.
103. Fitch, W.M. (1971). Towards defining course of evolution - minimum chnage for specific tree topology. Syst. Zool. *20*, 406.
104. Pagel, M. (1999). The maximum likelihood approach to reconstructing ancestral character states of discrete characters on phylogenies. Syst. Biol. *48*, 612–622.
105. Pirie, M.D., Humphreys, A.M., Antonelli, A., Galley, C., and Linder, H.P. (2012). Model uncertainty in ancestral area reconstruction: A parsimonious solution? Taxon *61*, 652–664.

Please cite this article in press as: Castañeda-Zárate et al., Food Reward Chemistry Explains a Novel Pollinator Shift and Vestigialization of Long Floral Spurs in an Orchid, Current Biology (2020), https://doi.org/10.1016/j.cub.2020.10.024

STAR★METHODS

KEY RESOURCES TABLE

REAGENT or RESOURCE	SOURCE	IDENTIFIER
Chemicals, Peptides, and Recombinant Proteins		
Diacetin (Glycerol diacetate)	Sigma-Aldrich	W500615; CAS: 25395-31-7
Tracetin (Glyceryl triacetate)	Sigma-Aldrich	90240; CAS: 102-76-1
Pentane	AMD CHROMASOLV®; Riedel-de-Haën	34894
C7-C40 Saturated Alkanes Standard	Sigma-Aldrich, SUPELCO	49452-U
Sudan IV	B. H. D. Laboratory Chemicals Group	NA
Methylene blue	Sigma-Aldrich	M9140; CAS: 7220-79-3
Critical Commercial Assays		
DNeasy® Plant Mini Kits	QIAGEN	Cat# 69104
Albumine, Bovine Serum, Fraction V, Fatty Acid-Free, Nuclease- and Protease-Free	Sigma-Aldrich, Calbiochem	126609; CAS: 9048-46-8
OneTaq® Quick-Load® Master Mix with Standard Buffer	New England Biolabs, Inc.	M0486S
Deposited Data		
Breeding system	This paper	http://doi.org/10.5281/zenodo.4044649
Day/Night pollinaria removals	This paper	http://doi.org/10.5281/zenodo.4044649
Morphometrics	This paper	http://doi.org/10.5281/zenodo.4044649
Natural fruit set	This paper	http://doi.org/10.5281/zenodo.4044649
Nectar volume and concentration	This paper	http://doi.org/10.5281/zenodo.4044649
Scent	This paper	http://doi.org/10.5281/zenodo.4044649
Floral color	This paper	http://doi.org/10.5281/zenodo.4044649
Spur shortening experiment	This paper	http://doi.org/10.5281/zenodo.4044649
ITS alignment	This paper	http://doi.org/10.5281/zenodo.4044649
Plastid alignment	This paper	http://doi.org/10.5281/zenodo.4044649
Software and Algorithms		
Geneious® 10.2.2.	Kearse et al.[74]	https://www.geneious.com/; RRID: SCR_010519
Mesquite 3.61	Maddison and Maddison[75]	http://www.mesquiteproject.org/; RRID: SCR_017994
MrBayes 3.2.7a	Ronquist et al.[76]	https://www.phylo.org/
NIST Spectral Library 2.0 g	Stein et al.[77]	https://www.nist.gov/system/files/documents/srd/NIST1a11Ver2-0Man.pdf
PAST 4.03	Hammer et al.[78]	http://folk.uio.no/ohammer/past/index.html
Primer v6	Clark and Gorley[79]	https://www.primer-e.com/
RStudio 3.6.3	Team[80]	https://rstudio.com/; RRID: SCR_000432
R package MASS 7.3-51.5	Venables and Ripley[81]	https://cran.r-project.org/web/packages/MASS/index.html
R package cvequality 0.1.3	Krishnamoorthy and Lee[82]	https://github.com/benmarwick/cvequality; RRID: SCR_019124
R package pavo 2.5.0	Maia et al.[83]	https://cran.r-project.org/web/packages/pavo/index.html; RRID: SCR_019123
IBM SPSS Statistics 26	IBM	https://www.ibm.com/products/spss-statistics?lnk=hpmps_bupr&lnk2=learn; RRID: SCR_019096
TNT 1.5	Goloboff and Catalano[84]	http://www.lillo.org.ar/phylogeny/tnt/; RRID: SCR_019122

(*Continued on next page*)

Please cite this article in press as: Castañeda-Zárate et al., Food Reward Chemistry Explains a Novel Pollinator Shift and Vestigialization of Long Floral Spurs in an Orchid, Current Biology (2020), https://doi.org/10.1016/j.cub.2020.10.024

Continued

REAGENT or RESOURCE	SOURCE	IDENTIFIER
Tracer v1.6	Rambaut et al.[85]	https://bioweb.pasteur.fr/packages/pack@Tracer@v1.6; RRID: SCR_019121
Ocean Optics SpectraSuite SpectroScopy Software	Ocean Optics	https://www.oceaninsight.com/products/software/
Other		
ITS GenBank accessions	This paper	https://www.ncbi.nlm.nih.gov/genbank/ Accession numbers: *BEE* (MT586319-MT586322), *MOTH1* (MT586330-MT586334), *MOTH2* (MT586344-MT586347), *MOTH3* (MT586375-MT586377), *MOTH4* (MT586402-MT586405), *MOTH5* (MT586423-MT586427)
Plastid GenBank accessions	This paper	https://www.ncbi.nlm.nih.gov/genbank/ trn*L* intron: *BEE* (MW053197-MW053200), *MOTH1* (MW053201-MW053205), *MOTH2* (MW053206-MW053209), *MOTH3* (MW053210-MW053212), *MOTH4* (MW053213-MW053216), *MOTH5* (MW053217-MW053221); trn*LF* intergenic spacer: *BEE* (MW053222-MW053225), *MOTH1* (MW053226-MW053230), *MOTH2* (MW053231-MW053234), *MOTH3* (MW053235-MW053237), *MOTH4* (MW053238-MW053241), *MOTH5* (MW053242-MW053246); trn*SG* intergenic spacer: *BEE* (MW053247-MW053250), *MOTH1* (MW053251-MW053255), *MOTH2* (MW053256-MW053259), *MOTH3* (MW053260-MW053262), *MOTH4* (MW053263-MW053266), *MOTH5* (MW053267-MW053271); mat*K*: *BEE* (MW053272-MW053275), *MOTH1* (MW053276-MW053280), *MOTH2* (MW053281-MW053284), *MOTH3* (MW053285-MW053287), *MOTH4* (MW053288-MW053291), *MOTH5* (MW053292-MW053296)

RESOURCE AVAILABILITY

Lead Contact

Further information and requests for resources should be directed to and will be fulfilled by the Lead Contact, Timotheüs van der Niet (vdniet@gmail.com).

Materials Availability

This study did not generate new unique reagents.

Data and Code Availability

Original data have been deposited in Zenodo (http://doi.org/10.5281/zenodo.4044649). DNA sequences can be downloaded from GenBank (https://www.ncbi.nlm.nih.gov/genbank/; ITS accession numbers: *BEE* (MT586319-MT586322), *MOTH1* (MT586330-MT586334), *MOTH2* (MT586344-MT586347), *MOTH3* (MT586375-MT586377), *MOTH4* (MT586402-MT586405), *MOTH5* (MT586423-MT586427). Plastid accession numbers, trn*L* intron: *BEE* (MW053197-MW053200), *MOTH1* (MW053201-MW053205), *MOTH2* (MW053206-MW053209), *MOTH3* (MW053210-MW053212), *MOTH4* (MW053213-MW053216), *MOTH5* (MW053217-MW053221); trn*LF* intergenic spacer: *BEE* (MW053222-MW053225), *MOTH1* (MW053226-MW053230), *MOTH2* (MW053231-MW053234), *MOTH3* (MW053235-MW053237), *MOTH4* (MW053238-MW053241), *MOTH5* (MW053242-MW053246); trn*SG* intergenic spacer: *BEE* (MW053247-MW053250), *MOTH1* (MW053251-MW053255), *MOTH2* (MW053256-MW053259), *MOTH3* (MW053260-MW053262), *MOTH4* (MW053263-MW053266), *MOTH5* (MW053267-MW053271); mat*K*: *BEE*

(MW053272-MW053275), *MOTH1* (MW053276-MW053280), *MOTH2* (MW053281-MW053284), *MOTH3* (MW053285-MW053287), *MOTH4* (MW053288-MW053291), *MOTH5* (MW053292-MW053296).

EXPERIMENTAL MODEL AND SUBJECT DETAILS

Study species and site

Plant species

The experimental subjects were populations of *Satyrium longicauda* Lindl. *Satyrium longicauda* (Orchidaceae) is a terrestrial orchid species, belonging to the subfamily Orchidoideae that is distributed in southern Africa.[17] In South Africa it is a common element of the grassland biome, occurring from near sea level up to 3100 m. Although the current taxonomy recognizes two subspecies,[17] extensive fieldwork has revealed the presence of many distinct forms, which often occur sympatrically. Most of these forms are known from multiple sites and are morphologically and genetically distinct (M.C.Z., unpublished data). Six of these forms co-occur at Mt Gilboa Nature Reserve (South Africa, 29°17'15.32"S, 30°17'34.61"E) (Figure S1). Population sizes of the forms vary from several dozen to hundreds of plants. The first forms start flowering in December, and the last form finishes flowering in April. Several forms co-flower (M.C.Z., unpublished data), but not all forms have overlapping flowering times. In addition to differences in flowering time, there are also differences in micro-habitat among some of the forms, although several forms can be found growing side by side. The main population of the *BEE* form, which is the central focus of this study, does not co-flower with any of the *MOTH* forms that grow in its immediate vicinity, but does overlap in flowering with the *MOTH1* form, which occurs several hundred meters distant (Figure S1).

Fieldwork took place during the flowering seasons of 2017-2019. Voucher specimens of the six forms are lodged in the Bews Herbarium (NU), University of KwaZulu-Natal, Pietermaritzburg campus (Table S1). Ezemvelo KZN Wildlife provided research permits for plant sampling (number OP4624/2018 and OP2302/2019).

Floral visitors

Insects visiting the experimental subjects were caught for identification and presence of pollinaria. Ezemvelo KZN Wildlife allowed insect catching through research permits (number OP2304/2019).

METHOD DETAILS

Pollination ecology

To confirm that all forms of *S. longicauda* need pollinators for fruit set,[21] between 6 (*MOTH3*) and 29 (*MOTH5*) randomly sampled inflorescences of each form were covered with a mesh bag prior to flowering during the flowering seasons of 2017 and 2018 respectively. For each plant, fruit set of a flower that was left unmanipulated was compared to fruit set of a flower that was cross-pollinated.

To characterize the pollination system of each form, we conducted pollinator observations. Observations were carried out while walking through populations of flowering individuals between 08 h00 and 20 h00 during 3-5 warm days and evenings per form. The total number of direct observation h was 84 (*BEE*), 55 (*MOTH1*), 30 (*MOTH2*), 43 (*MOTH3*), 41 (*MOTH4*), and 31 (*MOTH5*) respectively. Visitor behavior was recorded (including an assessment of whether visitors removed pollinaria) and visitors were captured for identification,[86] to measure the length of functional traits (proboscis and foreleg length), and to quantify pollinarium presence. The total number of captured pollinators was 15 (*BEE*), 6 (*MOTH1*), 16 (*MOTH3*), 6 (*MOTH4*), and 23 (*MOTH5*) respectively. No visitors were caught on *MOTH2*. To expand observation h, we also used motion trigger cameras (Bushnell NatureView HD Cam Model #: 119740, USA) to record flower visitors. The reliability of these cameras to record moth foraging activity in *S. longicauda* has recently been demonstrated.[26] This method is not suitable for recording visits by bees as these do not trigger cameras, presumably due to their small size and low temperature contrast between the insect body and relatively high ambient day-time temperatures. The total number of camera h was 360 (*BEE*), 502 (*MOTH1*), 264 (*MOTH2*), 378 (*MOTH3*), 364 (*MOTH4*), and 400 (*MOTH5*) respectively. The number of moth visitors captured on camera ranged from 3 (*BEE*) to 37 (*MOTH4*)

To distinguish whether pollination occurs during the day (consistent with bee pollination) or at night (consistent with moth pollination), we marked the bracts of flowers that had both pollinaria present with a permanent marker on between 10 (*MOTH1*, 2018) and 34 (*BEE*) inflorescences in 2018 (all forms) and 2019 (*MOTH1* and *MOTH2*). For *MOTH1* and *MOTH2* the experiment was run over two years (2018 and 2019), due to low visitation in 2018. Inflorescences were inspected for pollinarium removal at dusk and dawn for three to five consecutive days.[29] In cases where data were available for two years, these were pooled in the analysis (which was supported by a non-significant interaction between the factors 'time of day' and 'year').

Natural fruit set was determined during the flowering seasons of 2018 and 2019, respectively, for each form by counting the total number of fruits out of the total number of flowers produced for 30-50 randomly sampled inflorescences per form that were collected after flowering had finished.

Quantification of floral traits

Floral rewards

The presence of lipids (a constituent of floral oils) was assessed by rubbing small crystals of Sudan IV (B. H. D. Laboratory Chemicals Group, England) along the inner surface of the labellum of at least five flowers of each of the six forms.[35] We further tested for the presence of floral oil indirectly using a comparison of the amount of volatile acetylated glycerols in flowers of the six forms.[8] We immersed whole flowers in 3 mL of Pentane (AMD CHROMASOLV®,[3] 99%, Honeywell Riedel-de HaënTM, Germany) for 1 min to

obtain floral extracts (cf. Schäffler et al.[8]) from 5 inflorescences of the *BEE* form and 3-4 inflorescences of each of the *MOTH* forms. The same quantity of solvent was placed in empty vials as controls. The description of sample analysis using gas chromatography coupled with mass spectrometry (GCMS) is given below, following the description of the analysis of floral headspace samples.

To quantify differences in rewards among forms, we measured the volume of the nectar standing crop from all six forms of *S. longicauda* by piercing the tip of both spurs (they are too narrow to accommodate a micropipette) and gently drawing their content into a calibrated 5 μL capillary micropipette (ringcaps®, Hirschmann Laborgeräte, Germany). To determine sugar concentration, nectar was transferred to a refractometer designed for small nectar volumes (Eclipse 45–81; Bellingham and Stanley Ltd, Tunbridge Wells, Kent, UK). Sucrose percentage (°Brix) was converted to milligrams of sugar.[87] The number of samples varied among forms: *BEE* = 61, *MOTH1* = 31, *MOTH2* = 42, *MOTH3* = 32, *MOTH4* = 31, and *MOTH5* = 46.

Flower color

To determine whether forms of S. *longicauda* differ in flower color, we measured the spectral reflectance of the outer labellum surface and laterals sepals of five flowers randomly sampled from different individuals for each form. The spectral reflectance from 300 to 700 nm was obtained with an Ocean Optics S2000 spectrophotometer and fiber optic reflection probe (UV/VIS 400 μm). An Ocean Optics Mini-DT-2-GS Deuterium–Tungsten–Halogen with a spectral range of 200–2,000 nm was used as a light source. Each measurement was obtained after calibrating the spectra by using a diffuse reflectance standard (Ocean Optics WS-1) followed by spectra capture at 0.38 nm intervals using the Ocean Optics SpectraSuite SpectroScopy Software. For each perianth part the average from two measurements was used for analysis.

Morphology

To determine whether forms differ in morphometric traits, we sampled and measured at least 50 plants of each form (Table S1). A single flower from the middle third of each inflorescence was removed and 12 floral and vegetative traits counted or measured using a pair of digital calipers. The following traits were measured: plant height (from base to tip of inflorescence), inflorescence length, number of flowers, stem base diameter, inflorescence stem diameter at the base, length and width of largest leaf, galea aperture height, galea margin (lip flap) height, lateral sepal length, spur length (distance between the spur tip and the site of fusion with the galea), and functional spur length (spur tip to viscidium).

Floral scent

To quantify and compare scent composition among the six forms of *S. longicauda*, floral headspace samples were collected in the morning (~10 h00) and in the evening (~19 h00), coinciding with the peak of diurnal and nocturnal pollinator activity respectively. Floral headspace samples were collected from five randomly selected flowering individuals of each form in the field or in the laboratory. Sampling was done by placing each inflorescence in a polyacetate bag (Nalophan®, Kalle GmbH, Germany) and pumping the air through an adsorbent trap filled with 1 mg of Tenax® and 1 mg of Carbotrap® at a flow rate of 50 mL min^{-1}. After 30 min of pumping, traps were removed and placed separately inside labeled glass vials and stored at −20°C before analysis. To control for volatiles in the surrounding air, each sampling event also included a sample from an empty bag as described above.

Spur length

We assessed the average spur length among moth- and bee-pollinated *Satyrium* species. Species' pollination systems were based on literature.[22,29,38,88–90] We used the median value of spur length for each species for which pollinator data were available.[17]

To test for a difference in functionality in floral spurs between the *BEE* and a *MOTH* form, we set up an experiment in which we shortened the spurs to half their length. We bagged 20 plants in bud of the *BEE* form in December 2018 and 21 plants of the *MOTH3* form in January 2019 to prevent pollinator access. Once flowers had opened two different treatments were applied. On two flowers spurs were shortened by first gently squeezing them from the tip to move any nectar up, and then folding them at their halfway point. Folded spurs were fixed in that position by using thin (2mm) tape (cf. Ellis and Johnson[56]). A third flower was used as control. Spurs of this flower were not bent, but they were also gently squeezed and fixed with tape to control for manipulation effects. Pollinarium removal and the number of massulae deposited on stigmas were recorded after six days for the *BEE* form, and eight for the *MOTH3* form. Due to some browning of the stigmatic surface a 1% (w/v) solution of methylene blue (Sigma-Aldrich, USA) was used to facilitate counting of massulae.

Phylogenetic inference

DNA sampling and molecular procedure

To reconstruct phylogenetic relationships among the forms of *S. longicauda*, we used an existing framework of species-level phylogenetics that has previously been used in *Satyrium*.[53,91] We used DNA sequences from the nuclear ribosomal internal transcribed spacer (nrITS), which is particularly variable in Orchidaceae and provides resolution at the species level.[92] Given previously detected topological incongruence between datasets from different genomic partitions,[91] we supplemented nuclear data with DNA sequences from the plastid genome, using the *mat*K gene, and the *trn*LF and *trn*SG regions.[93]

We collected foliar tissue from 3-5 individuals of each form and dried this on silica prior to DNA extraction. DNA was isolated using the DNeasy® Plant Mini Kits (QIAGEN, Hilden, Germany). Amplification of the ITS region was carried out using the primers ITS5 and ITS4,[94] whereas the *trn*LF region was amplified using primers trnLF c and trnLF f.[95] The primers trnG and trnS were used to amplify the *trn*SG region,[93] and the plastid gene *mat*K was amplified using the matK −19F and matK R1 primers.[96] The polymerase chain reaction (PCR) for the ITS region was performed using a mix composed of 12.5 μL of OneTaq® Quick-Load® Master Mix with Standard Buffer (New England Biolabs), 1 μL bovine serum albumin (10 ng/μL), 0.5 μL of each primer (100 ng/μl), 10.5 μL distillated H_2O, and 1 μL of extracted DNA (c. 100 ng). Amplification was carried out in a Veriti 96-Well Thermal Cycler following a PCR method that

Please cite this article in press as: Castañeda-Zárate et al., Food Reward Chemistry Explains a Novel Pollinator Shift and Vestigialization of Long Floral Spurs in an Orchid, Current Biology (2020), https://doi.org/10.1016/j.cub.2020.10.024

included an initial 30 s of denaturation at 94°C, followed by 35 cycles of 30 s denaturation at 94°C, 1 min annealing at 53°C, 1 min extension at 68°C, finished with final extension of 7 min at 68°C. The plastid regions were amplified following protocols used previously in the genus *Satyrium*.[53,91] All PCR reactions were performed in a total volume of 25 μL. The PCR products were purified and sequenced using Sanger sequencing, implementing BigDye chemistry, either at the Central Analytic Facilities (CAF) of Stellenbosch University (South Africa), or at Macrogen Europe (the Netherlands).

QUANTIFICATION AND STATISTICAL ANALYSIS

Timing of pollination

The number of removed pollinaria out of the total number of pollinaria available per flower was compared between day and night periods for each form using generalized estimating equations (GEE) with a binomial distribution and a logit link function in SPSS 26 (IBM Corp.) To control for repeated-measures on the same subject (plant) over time we implemented an autoregressive correlation matrix.[29] We specifically tested whether the timing of pollinarium removal interacted with form (form × time of removal). Estimated marginal means and standard errors were back-transformed from the logit scale, resulting in asymmetrical error bars. Pairwise comparisons were implemented using Sequential Šidák correction.[97]

Floral trait quantification

Rewards

Nectar volume and sugar quantity between forms were both compared using generalized linear models (GLM) with a normal distribution and an identity link function in SPSS 26 (IBM Corp.). The Sequential Šidák correction method was used for multiple pairwise comparisons among forms.[97]

Flower color

For visualization purposes we calculated the color loci of the flower colors in a color hexagon based on honeybee vision.[98] This approach may also provide insight into the question whether the bee species *Rediviva neliana* can discriminate color among forms of *S. longicauda*, as hymenopteran vision systems are relatively conserved.[99] Because no differences in color were observed between the labellum and sepals, we only used the labellum values and plotted these in the bee color hexagon using the R package *pavo* 2.5.0.[83]

Morphology

To visualize differences in morphometric traits between the six forms we implemented a Linear Discriminant Analysis (LDA) on 322 individuals with the *lda* function from the MASS package version 7.3-51.5[81] using RStudio 3.6.3.[80]

To quantify whether morphometric traits vary among forms we performed a one-way permutational multivariate analysis of variance (PERMANOVA) using form as factor. For this analysis we first calculated pairwise Euclidean distances among all individuals of all forms. Because measurements are on a different scale, we standardized the dataset by subtracting the mean and dividing by the standard deviation before calculating Euclidean distance. Distance calculation and PERMANOVA were performed in the software package PAST Version 4.03.[78]

To determine whether the *BEE* form differs more from *MOTH* forms than *MOTH* forms do from each other, we contrasted mean pairwise comparisons of morphological distance. Distances were averaged for comparisons between individuals of each possible pairwise comparison between forms. This resulted in five comparisons between the *BEE* and five *MOTH* forms, and ten comparisons among the five moth forms. We then used GLM with a Gaussian distribution and an identity link function in SPSS 26 (IBM Corp.) to compare whether pairwise differences vary for 'between pollination system' versus 'within pollination system' comparisons.

Chemical analysis

Volatiles were characterized and quantified using GCMS. Traps were analyzed using a Varian CP-3800 gas chromatograph (Varian, Palo Alto, California, USA) with an Alltech EC-WAX column (30 m × 0. 25 mm internal diameter × 0.25 μm) coupled to a Bruker 300-MS quadrupole mass spectrometer in electron-impact ionization mode. Traps were placed in a Varian 1079 injector equipped with a Chromatoprobe thermal desorption device.[100] The flow of helium carrier gas was 1 mL min^{-1}. For thermodesorption, the injector was held at 40°C for 2 min with a 20:1 split and then increased to 200°C at 200°C min^{-1} in splitless mode. Meanwhile, the gas chromatograph oven was held at 40°C for 3 min and then ramped up to 240°C at 10°C min^{-1} and held there for 12 min.[29] Quantification of emission rates was done by injecting a known amount of methyl benzoate and run it using the same temperature program. The resulting peak area in the chromatogram was calibrated and compared to the total peak area of samples.[29]

Compound identification was done by comparing mass spectra and the Kovats Retention Index (based on comparison of compound retention times to those of a set of alkanes) to published values using the Bruker Workstation software Version 7.0 in combination with the NIST Mass Spectral Program for the NIST Spectral Library Version 2.0 g.[77] This approach resulted in identification of most peaks. Peaks that could not be identified were scored as unknown, with the six most dominant mass fragments indicated. Quantification of compounds was based on integrating the area under peaks in chromatograms.

Comparison of scent samples taken among forms during both day and night was done using 2-way PERMANOVA in the software PAST 4.03,[78] testing for an effect of time of sampling (day/night), form, and the interaction between these two factors. The comparison of differences among and within pollinator group comparisons followed the same procedure as was done for the morphometrics dataset, although this test was done separately for the set of samples taken during day and evening respectively. To compare scent profiles of samples we first applied square-root transformation to the proportion of identified compounds, to downweight the

Please cite this article in press as: Castañeda-Zárate et al., Food Reward Chemistry Explains a Novel Pollinator Shift and Vestigialization of Long Floral Spurs in an Orchid, Current Biology (2020), https://doi.org/10.1016/j.cub.2020.10.024

influence of dominant compounds, and then calculated Bray-Curtis similarity. For the comparison of average Bray-Curtis similarity between *BEE* and *MOTH* forms versus among *MOTH* forms, we logit-transformed the average Bray-Curtis similarity as these values are bounded between 0 and 1. For visualization of variation among samples we plotted these using non-metric multidimensional Scaling (NMDS) in PAST 4.03.[78]

To quantify which compounds are most characteristic for each form, we used a similarity percentage (SIMPER) analysis, focusing on compounds that had a cumulative contribution to 50% similarity. This analysis was done for day and evening samples separately, based on Bray-Curtis similarity of square-root transformed proportions of compounds in the software Primer v6.[79]

The presence of volatile acetylated glycerols was quantified by placing 5 μL of floral pentane extract in a quartz vial and inject this into a SCION 436-GC with a SGE SolGel Wax polar column (30 m × 0.25 mm internal diameter × 0.25 μm film thickness) coupled to a SCION SQ (Livingston, UK) using the same temperature method as was used for the headspace samples, but with an additional back-up step holding the temperature at 260°C during 25 min at 20°C min^{-1} to bake out the column to remove possible residual compounds that are part of the direct flower extract. Acetylated glycerol compounds were identified and quantified based on comparison with synthetic standards. For both diacetin and triacetin, 2 μL was placed in a quartz vial and injected under identical conditions as described above. The chromatograms were used to calculate peak area per mass. This information was used to calculate how much of each of these two compounds was present per flower. Other compounds associated with oil-producing flowers were identified based on their highly characteristic mass spectrum and Kovats Retention Indices that were calculated against a set of alkanes run under the same temperature conditions using the MS Workstation software Version 8.0.1 with the NIST Mass Spectral Program for the NIST Spectral Library Version 2.0 g.[77] The quantity of other compounds was calculated by averaging the peak area per mass for diacetin and triacetin as a reference. None of the control samples that were obtained without flowers showed any signs of acetylated glycerols or other compounds related to oil production.

To compare amounts of volatiles associated with oil production, we integrated the area under each peak and compared the quantity between the *BEE* and *MOTH* forms. This comparison was done using GLM in SPSS 26 (IBM Corp.) implementing a Gamma distribution with a log link function, with pollinator as predictor and form nested inside pollinator. For two samples of the moth forms, no triacetin was detected. To allow the model to run we replaced a 0 with a value of 1.0^{-10}, which makes the test slightly more conservative.

Spur length variation and functionality

To test whether spur length (measured from the tip to where they merge with the labellum) varies among forms, we used GLM implementing a Gaussian distribution with an identity link function. Pairwise comparisons were done by implementing the Sequential Šidák procedure in SPSS 26 (IBM Corp.).[97]

To test whether the coefficient of variation in spur length is greater in the *BEE* form than the *MOTH* forms (as a signature of relaxed selection) we calculated a coefficient of variation of spur length based on the measurements described above and compared these using the modified signed-likelihood ratio test[82] in the R package *cvequality* version 0.1.3.[101] To assess whether the observed pattern is unique for spur length (specifically indicating relaxed selection in the *BEE* form for this particular character), we repeated this analysis for the character lateral sepal length.

To test for an effect of spur bending on male fitness (pollinarium removal) and female fitness (number of massulae deposited on the stigmas), we analyzed the data using GEE with plant as a subject. For pollinarium removal (number of pollinaria removed out of number present) we implemented a binomial distribution with logit link function and for number of massulae deposited we implemented a negative binomial distribution with a log link function in SPSS 26 (IBM Corp.). We tested whether there was an interaction between treatment and form, and compared marginal means within forms using the Sequential Šidák procedure.[97] Estimated marginal means and standard errors were back-transformed to the original scale and plotted as asymmetrical error bars.

Phylogenetic analyses and ancestral character state reconstruction

Sequence alignment and phylogenetic analyses

DNA sequence electropherograms were edited and assembled with Geneious® 10.2.2.[74] Sequences were then aligned by eye with the matrix previously used for a species-level phylogenetic analysis of *Satyrium*.[91] Phylogenetic relationships were inferred from nuclear and plastid sequences separately through maximum parsimony and Bayesian Inference. The parsimony search started with 10,000 random-addition sequence replicates of Wagner trees, retaining 100 trees per replication, followed by tree bisection-reconnection (TBR) branch swapping, performed in TNT 1.5.[84] Bootstrap resampling was used to evaluate support of the nodes of the most parsimonious tree.[102] Results of 10,000 replicates were summarized using absolute frequencies for each group. Bayesian analyses were conducted in the program MrBayes version 3.2.7[76] on the CIPRES Science Gateway using default settings. The evolutionary models were selected according to a previous analysis.[91] Searches consisted of five million generations with chain sampling every 1,000 generations. The first 20% of generations was discarded as burn-in. Convergence was confirmed by evaluating whether the Effective Sample Size of all estimated parameters was above 200 in Tracer v1.6.[85] After removing the burn-in generations, each 8^{th} tree was selected from each of the two treefiles and combined for a dataset of 1,000 trees that was used for ancestral character state reconstruction.

Ancestral character state reconstruction

To polarize the direction of the pollinator shift and reconstruct the evolution of floral oil we implemented ancestral character state reconstruction. Prior to this we omitted taxa not relevant for this analysis. The final matrix included all *S. longicauda* accessions from Mt Gilboa, as well as a further seven species of *Satyrium*, sampled for the presence of acytelated glycerols (see below), which

Please cite this article in press as: Castañeda-Zárate et al., Food Reward Chemistry Explains a Novel Pollinator Shift and Vestigialization of Long Floral Spurs in an Orchid, Current Biology (2020), https://doi.org/10.1016/j.cub.2020.10.024

were chosen as representatives of the main clades of *Satyrium* (see Figure S3 and[91] for information on GenBank accession numbers). These species include the two varieties of *S. cristatum*, *S. macrophyllum*, *S. microrrhynchum*, *S. neglectum* ssp. *neglectum*, *S. parviflorum*, *S. rhynchanthum*, *S. sphaerocarpum*, and *S. trinerve*. In case multiple accessions were available for a species or form, we randomly selected a single individual per form or species per generation from the set of 1,000 trees for inclusion in the trees used for ancestral character state reconstruction. We performed both parsimony and likelihood-based analyses of ancestral character state reconstruction, but focus mainly on the parsimony results using Fitch parsimony.[103] The rationale is that under certain conditions, especially if evolutionary change is infrequent, model-based approaches can return counter-intuitive results (see Figure 3 in Pagel[104]). A preliminary analysis implementing Bayesian ancestral character state reconstruction confirmed that our dataset is similar to the case discussed in Pagel.[104] In such cases, parsimony may outperform model-based approaches.[105] Furthermore, model-based approaches are particularly useful in datasets with long branches (where multiple changes per branch, which cannot be modeled with parsimony, are expected). However, our focus is on reconstructing character evolution within a recently evolved species complex, where branches are relatively short. We first reconstructed the ancestral pollinator in the *S. longicauda* species complex. We coded each form by its primary pollinator (moth versus oil-collecting bee). We then performed ancestral character state reconstruction on the set of trees retrieved from the Bayesian phylogenetic analysis using the 'Trace Character over Trees' command in Mesquite 3.61.[75] These analyses were done separately for the trees resulting from the phylogenetic analysis of plastid and nuclear DNA sequences respectively. For the plastid analysis, one of the *MOTH* forms was excluded for this analysis, as it was not part of the clade that comprises the *BEE* form and most other *MOTH* forms. We performed likelihood-based analyses in Mesquite, using the MK1 model.[104]

We also traced the evolution of floral oil in *Satyrium*. For this analysis we first took floral extracts of six of the seven species mentioned above (apart from *S. rhynchanthum*) according to the methods described above for *S. longicauda*. We then coded each species for oil presence or absence. For *S. rhynchanthum*, which is pollinated by *Rediviva gigas*,[38] we confirmed the presence of diacetin in a floral headspace sample (T.N., unpublished results). The evolution of floral oil was analyzed using the same method as described for pollinator.

Current Biology, Volume *31*

Supplemental Information

Food Reward Chemistry Explains a Novel Pollinator Shift and Vestigialization of Long Floral Spurs in an Orchid

Miguel Castañeda-Zárate, Steven D. Johnson, and Timotheüs van der Niet

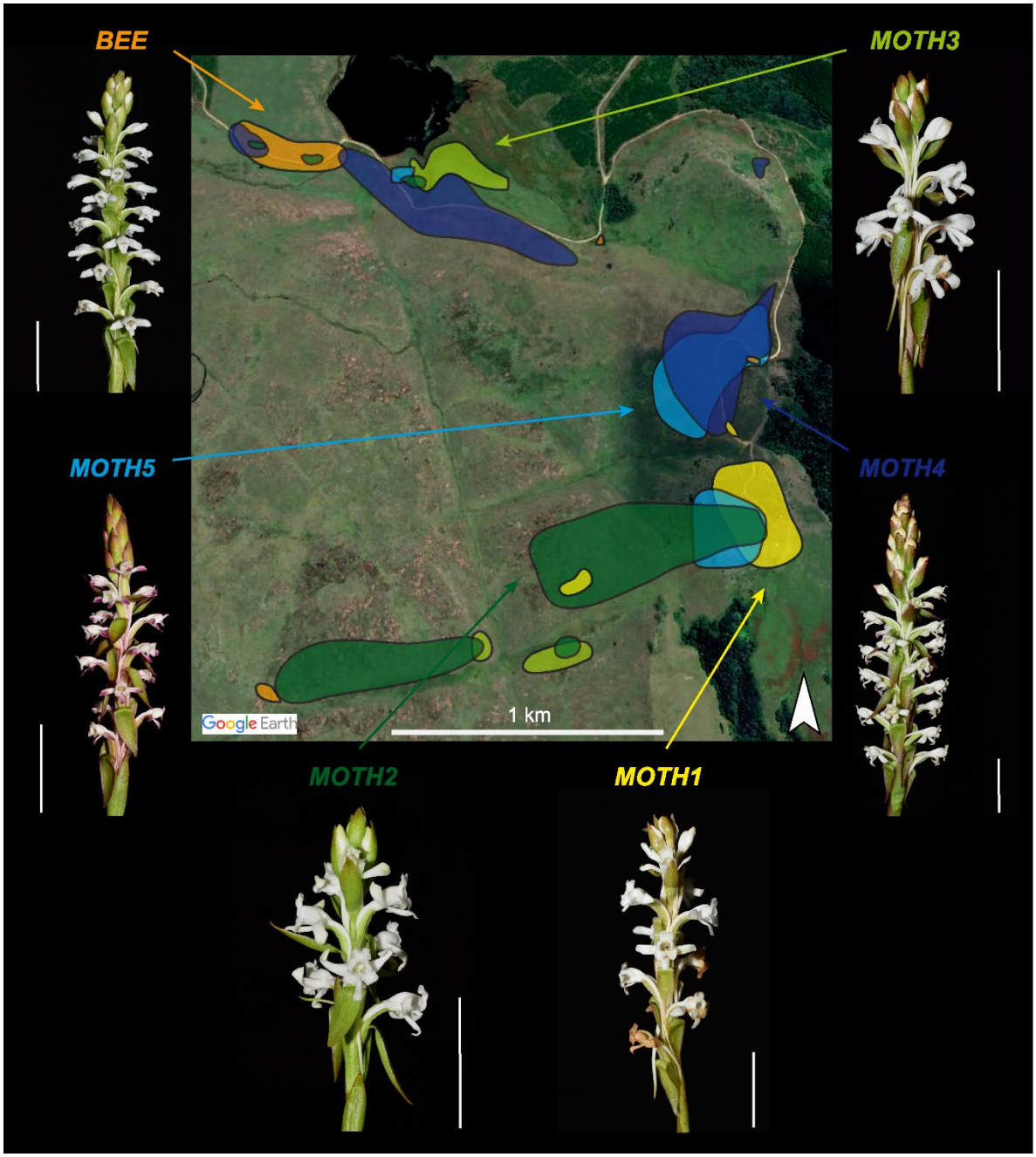

Figure S1. Map with approximate distribution of the six forms used in this study.

Related to STAR methods. Scale bar = 50 mm.

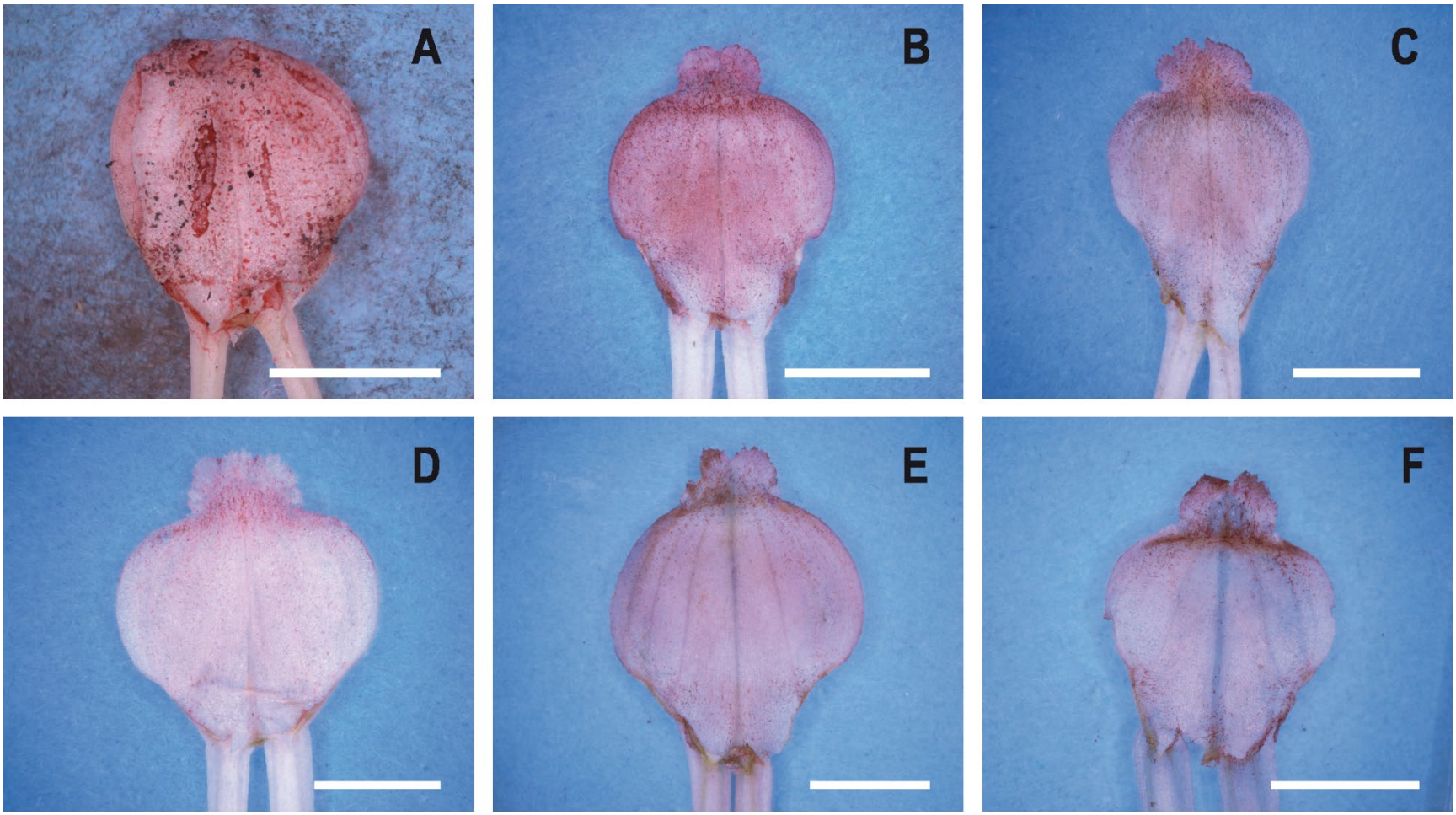

Figure S2. Inside labellum surface stained with Sudan IV crystals. Related to Figure 2. (A) *BEE*, (B) *MOTH1*, (C) *MOTH2*, (D) *MOTH3*, (E) *MOTH4*, (F) *MOTH5*. Scale bar = 5 mm.

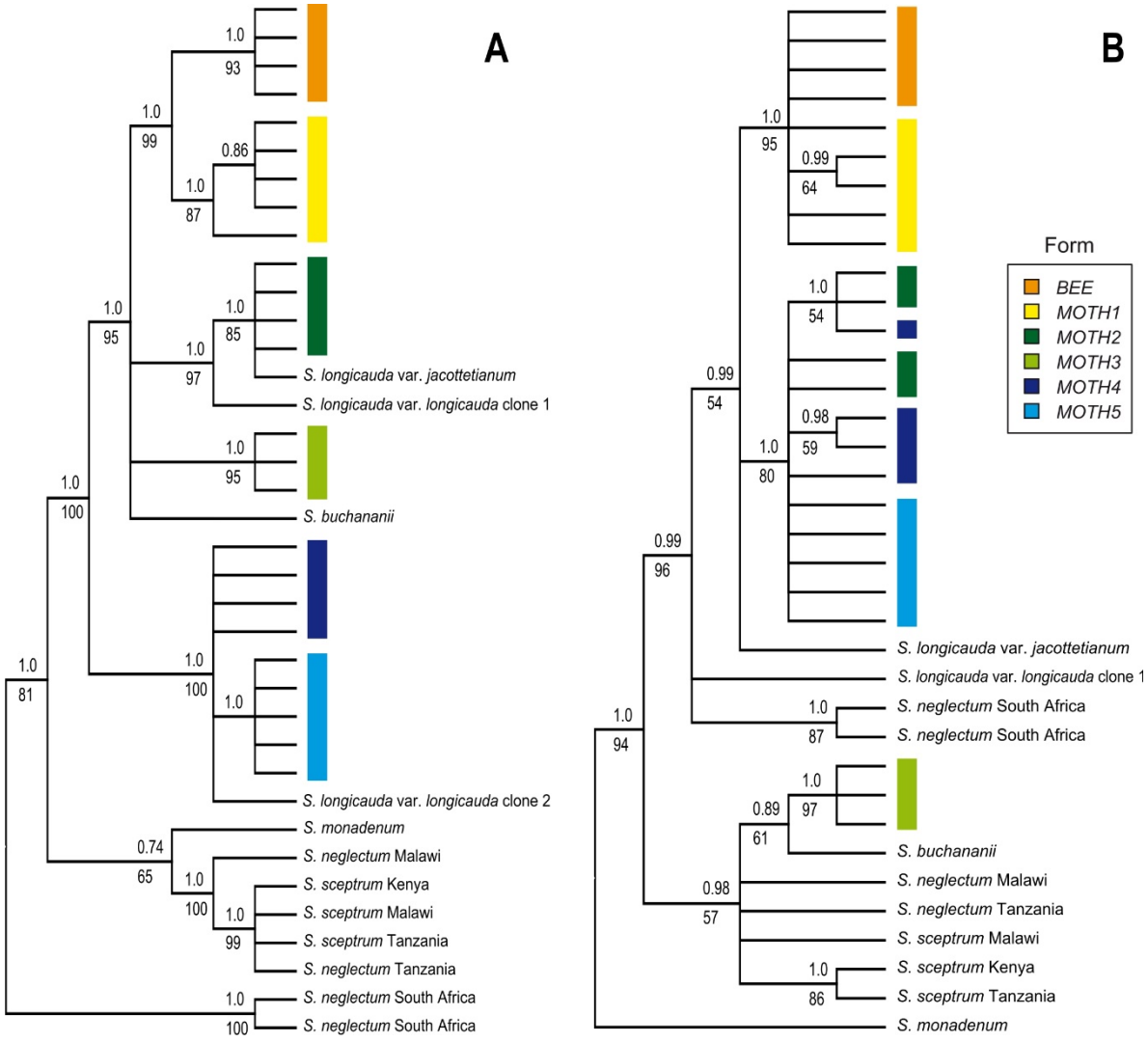

Figure S3. Majority rule consensus trees of Bayesian inference of *Satyrium longicauda* and closely related taxa based on (A) nuclear and (B) chloroplast DNA sequences.

Related to Figure 4. Parsimony bootstrap values are given above branches, Bayesian posterior probability values are given below the branches. Taxon names refer to [79]. The *BEE* form is coded in orange and is well-supported to be sister to *MOTH1* in both topologies.

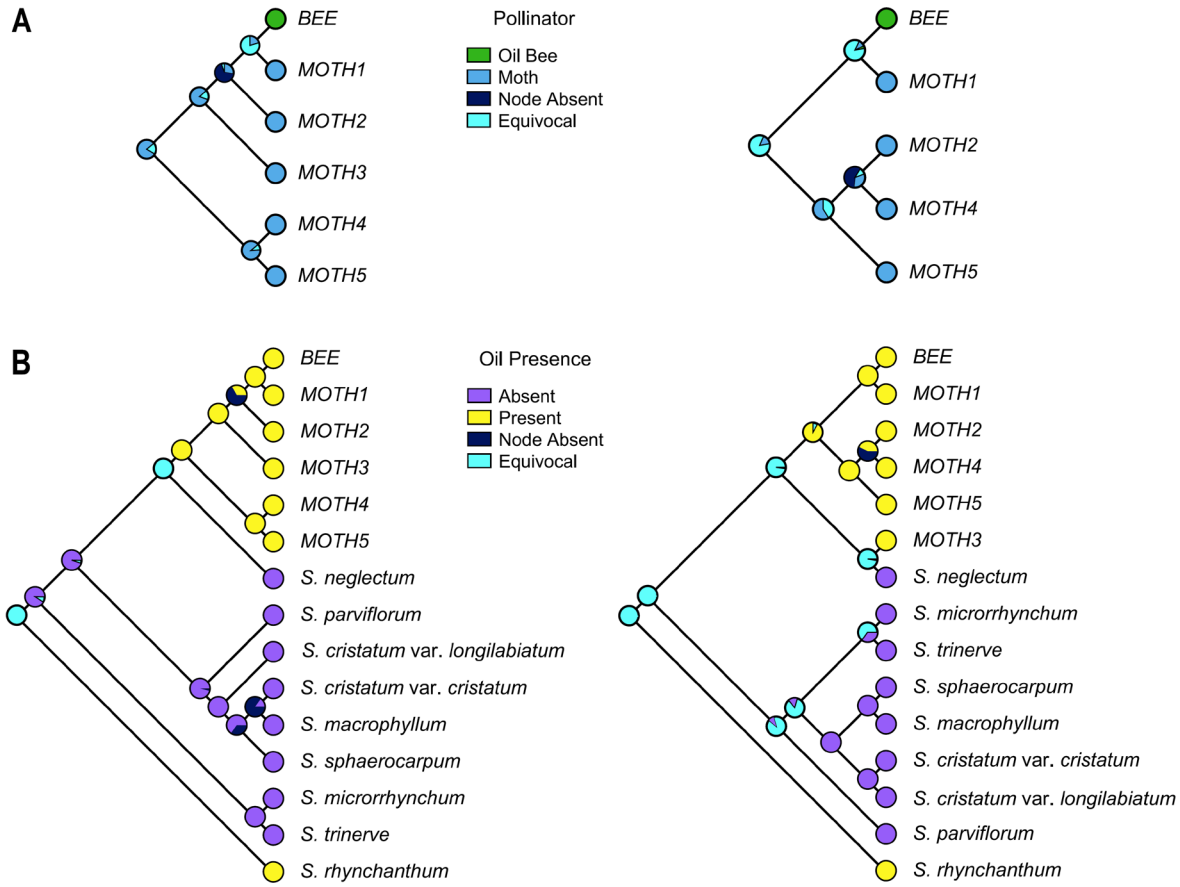

Figure S4. Ancestral character state reconstruction of (A) pollinator (*Satyrium longicauda* complex only) and (B) diacetin (*Satyrium*). Related to Figure 4. Results are obtained using maximum likelihood reconstruction and mapped onto a randomly chosen tree from Bayesian inference of nuclear (left) and plastid (right) DNA sequences.

Species	Form	N (n)	Collection number
Satyrium longicauda Lindl.	*BEE*	50 (5)	1412, 1414, 1488, **1494**, 1606, 1614
	MOTH1	50 (3)	1490, **1495**, 1612, 1622
	MOTH2	53 (4)	1413, 1508, **1613**
	MOTH3	69 (4)	1415, 1426, **1523**, 1620, 1635
	MOTH4	50 (4)	1425, 1444, **1537**, 1547, 1634
	MOTH5	50 (4)	1443, 1452, 1453, **1641**, 1657
Satyrium cristatum Sond. var. *cristatum*		1	**1557**
Satyrium cristatum var. *longilabiatum* A.V. Hall		1	**1528**
Satyrium macrophyllum Lindl.		3	**1556**, **1567**, **1568**
Satyrium microrrhynchum Schltr.		2	**1549**
Satyrium neglectum Schltr.		2	**1530**, **1553**
Satyrium parviflorum Sw.		2	**1524**, **1531**
Satyrium sphaerocarpum Lindl.		1	**1534**
Satyrium trinerve Lindl.		1	**1554**

*Samples were collected by the first author under the acronym of MCZ. Voucher specimens are housed in the UKZN's Bews Herbarium (NU), Pietermaritzburg, South Africa.

Table S1. Voucher table of *Satyrium longicauda* forms and other *Satyrium* species measured for acytilated glycerols. Related to STAR methods. Sample sizes of individuals measured for morphometrics and oil presence (between brackets) are provided. Collection numbers in bold refer to the collection used to obtain floral solvent extracts.

Form	Species	Individuals observed directly (number with pollinaria)	Individuals recorded on camera (number with pollinaria)	Mean number of pollinaria (range)	Proboscis length (mean±SD)
BEE	**HYMENOPTERA**				
	Melittidae				
	Rediviva neliana Cockerell	134 (84)	2 (1)	4 (1-12)	—
	Apidae				
	Xylocopa sp.	1 (0)	—	—	—
	LEPIDOPTERA				
	Pieridae				
	Colotis eris Klug	1 (0)	1 (0)	—	—
	Nymphalidae				
	Unidentified	1 (0)	—	—	—
	Noctuidae				
	Unidentified	1 (0)	—	—	—
MOTH1	**LEPIDOPTERA**				
	Sphingidae				
	Basiothia schenki (Möschler)	—	3 (1)	—	—
	Hippotion celerio (Linnaeus)	1 (1)	—	—	—
	Noctuidae				
	Cucullia hutchinsoni Hampson	3 (1)	—	5	32.79
	Cucullia terensis Felder & Rogenhofer	1 (0)	—	—	28.4
	DIPTERA				
	Nemestrinidae				
	Prosoeca sp.	6 (4)	—	1.17 (1-3)	25.1
	Tabanidae				
	Philoliche aethiopica Thunberg	1 (1)	—	1	15.8
MOTH2	**LEPIDOPTERA**				
	Sphingidae				
	Basiothia schenki (Möschler)	2 (1)	3 (2)	—	—
	Noctuidae				
	Cucullia hutchinsoni Hampson	1 (1)	1 (0)	1	—
MOTH3	**LEPIDOPTERA**				
	Sphingidae				
	Basiothia schenki (Möschler)	87 (27)	7 (5)	3.17 (1-7)	40.68±1.24
	Hippotion celerio (Linnaeus)	1 (1)	1 (1)	—	—
	Hippotion osiris (Dalman)	—	1 (1)	5	—
	Noctuidae				
	Cucullia hutchinsoni Hampson	20 (5)	8 (2)	2.70 (1-6)	32.4±1.27
	Cucullia terensis Felder & Rogenhofer	1 (0)	—	—	26.9
	Pieridae				
	Colotis eris Klug	1 (0)	—	—	—
	DIPTERA				
	Nemestrinidae				
	Prosoeca sp.	5 (0)	—	—	26.45±3.00
MOTH4	**LEPIDOPTERA**				
	Sphingidae				
	Agrius convolvuli (Linnaeus)	2 (1)	—	1	91.22
	Basiothia schenki (Möschler)	59 (27)	26 (18)	2.40 (1-7)	41.08±2.63
	Noctuidae				
	Cucullia hutchinsoni Hampson	20 (13)	11 (3)	—	—
	Unidentified	1 (0)	—	—	—

	LEPIDOPTERA				
	Sphingidae				
	Basiothia schenki (Möschler)	1 (0)	—	—	—
	Hippotion eson (Cramer)	1 (0)	—	—	45.08
	Hyles livornica (Esper)	1 (1)	—	1	28.81
MOTH5	Noctuidae				
	Cucullia chrysota Hampson	2 (1)	—	4	26.78±5.96
	Cucullia hutchinsoni Hampson	70 (41)	14 (9)	2.57 (1-4)	31.88±1.70
	Cucullia terensis Felder & Rogenhofer	2 (1)	—	4	28.01±0.71
	Thysanoplusia orichalcea (Fabricius)	2 (1)	—	1	16.16±1.87
	Unidentified	1 (0)	—	—	17.41
	Unidentified	1 (0)	—	—	7.21

Table S2. Insects observed visiting *Satyrium longicauda.* Related to Figure 1. Visitors are grouped by family within their respective order. Proboscis length is given in millimetres.